Mapping the anisotropies of Stochastic gravitational-Wave Background with Ground-Based Detectors

Jishnu Suresh
Université catholique de Louvain

Data analysis challenges for stochastic gravitational wave backgrounds
CERN, July 19-21, 2023

STOCHASTIC GRAVITATIONAL WAVE BACKGROUND

Superposition of signals too weak or too numerous to individually detect

Looks like noise in a single detector

Characterized statistically in terms of moments (ensemble averages) of the metric perturbations

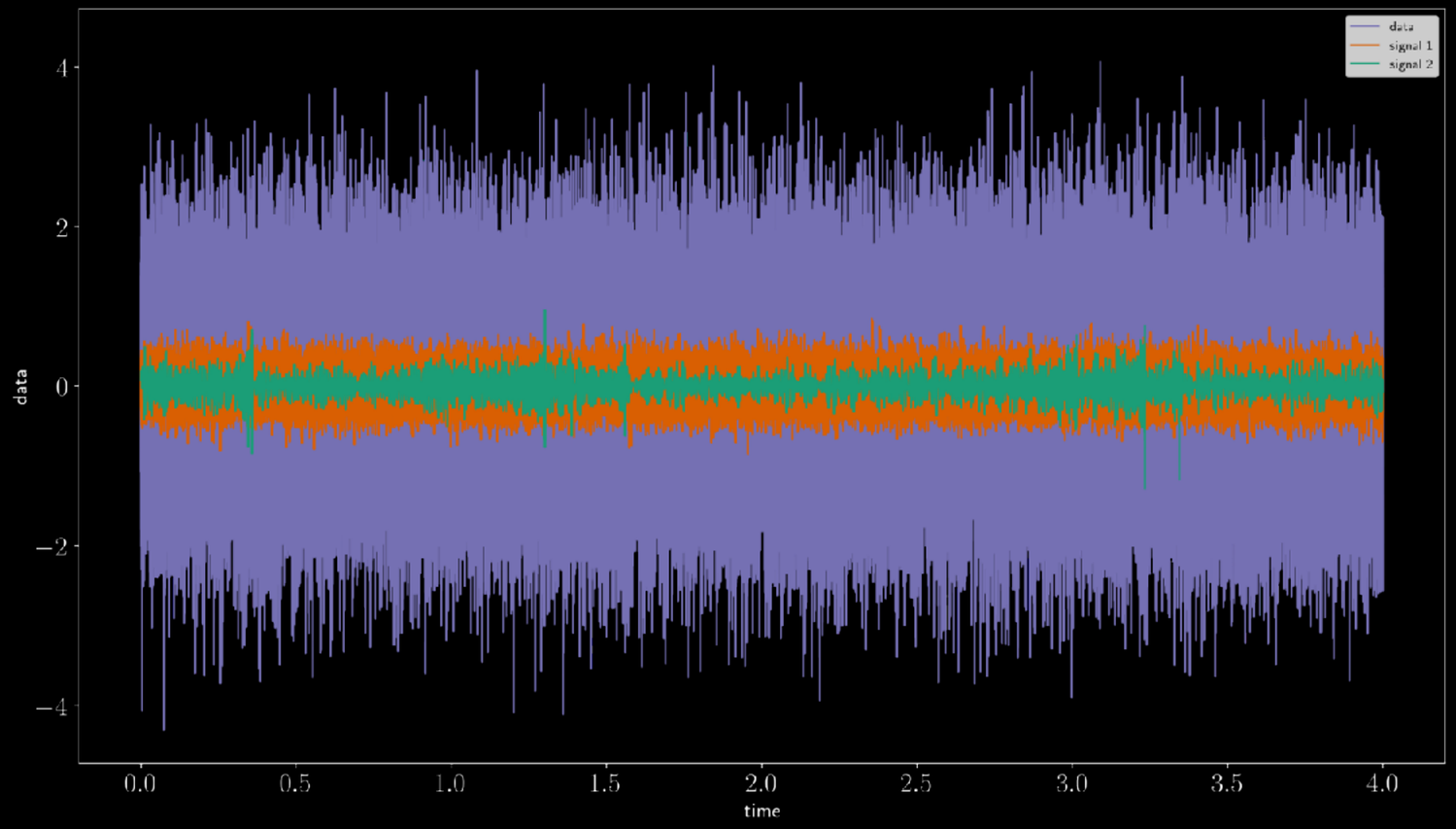

STOCHASTIC GRAVITATIONAL WAVE BACKGROUND

In this talk, we will only consider the following cases

Unpolarized,

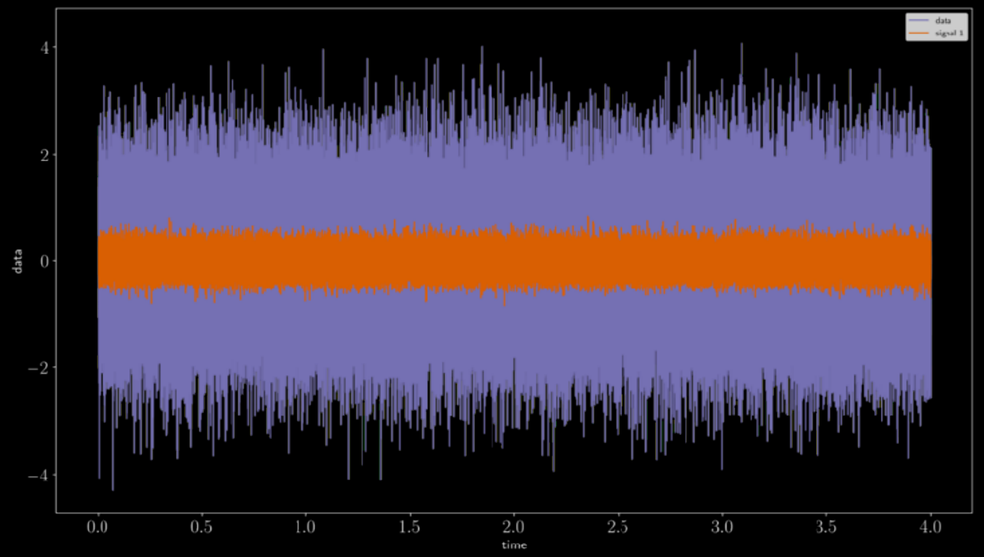

,

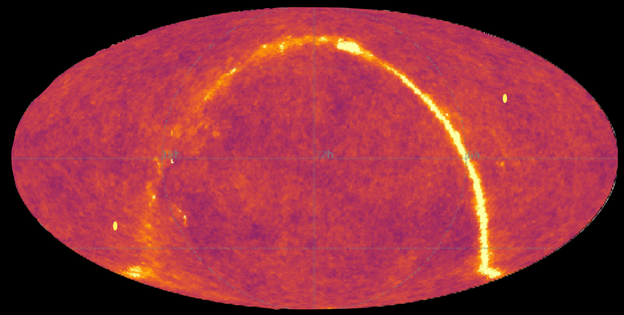

Unpolarized, stationary, anisotropic:

$$\langle h_A(f,\hat{n})\, h^*_{A'}(f',\hat{n}')\rangle = \frac{1}{4}\mathscr{P}(f,\hat{n})\,\delta(f-f')\delta_{AA'}\,\delta^2(\hat{n},\hat{n}')$$

ANISOTROPIES IN THE SGWB

—> Anisotropic distribution of the emitting sources.

—> Due to propagation: as gravitational-wave propagate, they accumulate line-of-sight effects, crossing different matter density fields which are inhomogeneously distributed in the Universe.

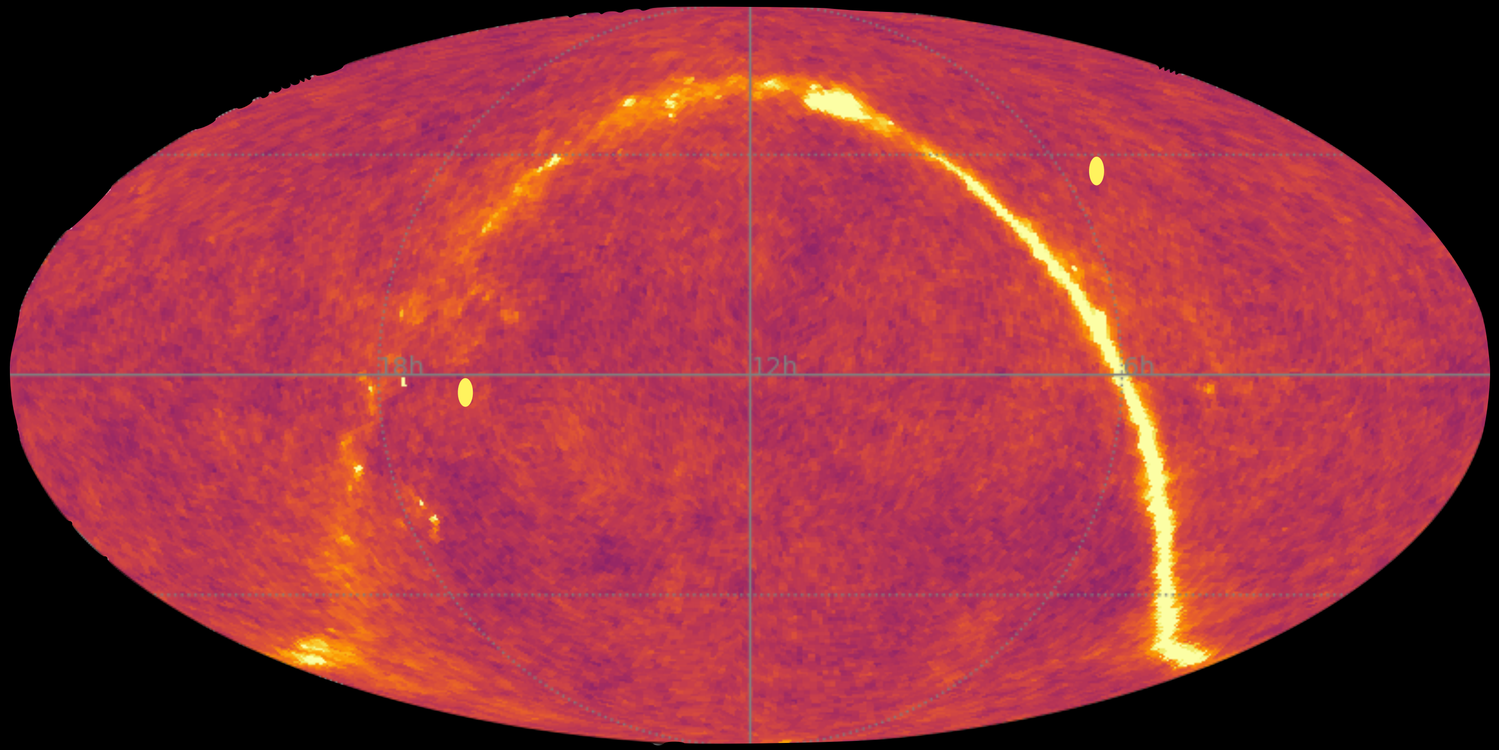

SGWB anisotropies will have the imprints of the matter structures in the universe*

*See Vuk's talk

WHAT DETECTION METHODS CAN WE USE?

See Joe's talk for details

The stochastic signal looks more like noise in a single detector.

What can be done:

- Identify features that distinguish between the expected signal and noise.
- Detectors with uncorrelated noise: cross-correlation separates the signal from the noise.

Data from two detectors: $d_1 = h + n_1 \qquad d_2 = h + n_2$ h – > common GW signal component

Cross-correlation: $\langle d_1\, d_2 \rangle = \langle h^2 \rangle + \langle n_1\, n_2 \rangle + \langle h\, n_2 \rangle + \langle n_1\, h \rangle = \langle h^2 \rangle + \langle n_1\, n_2 \rangle$ ($\langle h\, n_2 \rangle \to 0$, $\langle n_1\, h \rangle \to 0$)

Assuming detector noise is uncorrelated*: $\langle d_1\, d_2 \rangle = \langle h^2 \rangle + \langle n_1\, n_2 \rangle$ ($\langle n_1\, n_2 \rangle \to 0$)

$$\langle d_1\, d_2 \rangle = \langle h^2 \rangle \equiv S_h$$

Cross-correlation separates the signal from the noise

Intensity of the background

*Correlated noise and anisotropy SV+ (in-preparation)

HOW DO WE MAP THE SGWB SKY?

How do we extract the anisotropic SGWB signal from the ground-based interferometer data?

How to solve for its directionality?

How do we effectively map this signal on the sky?

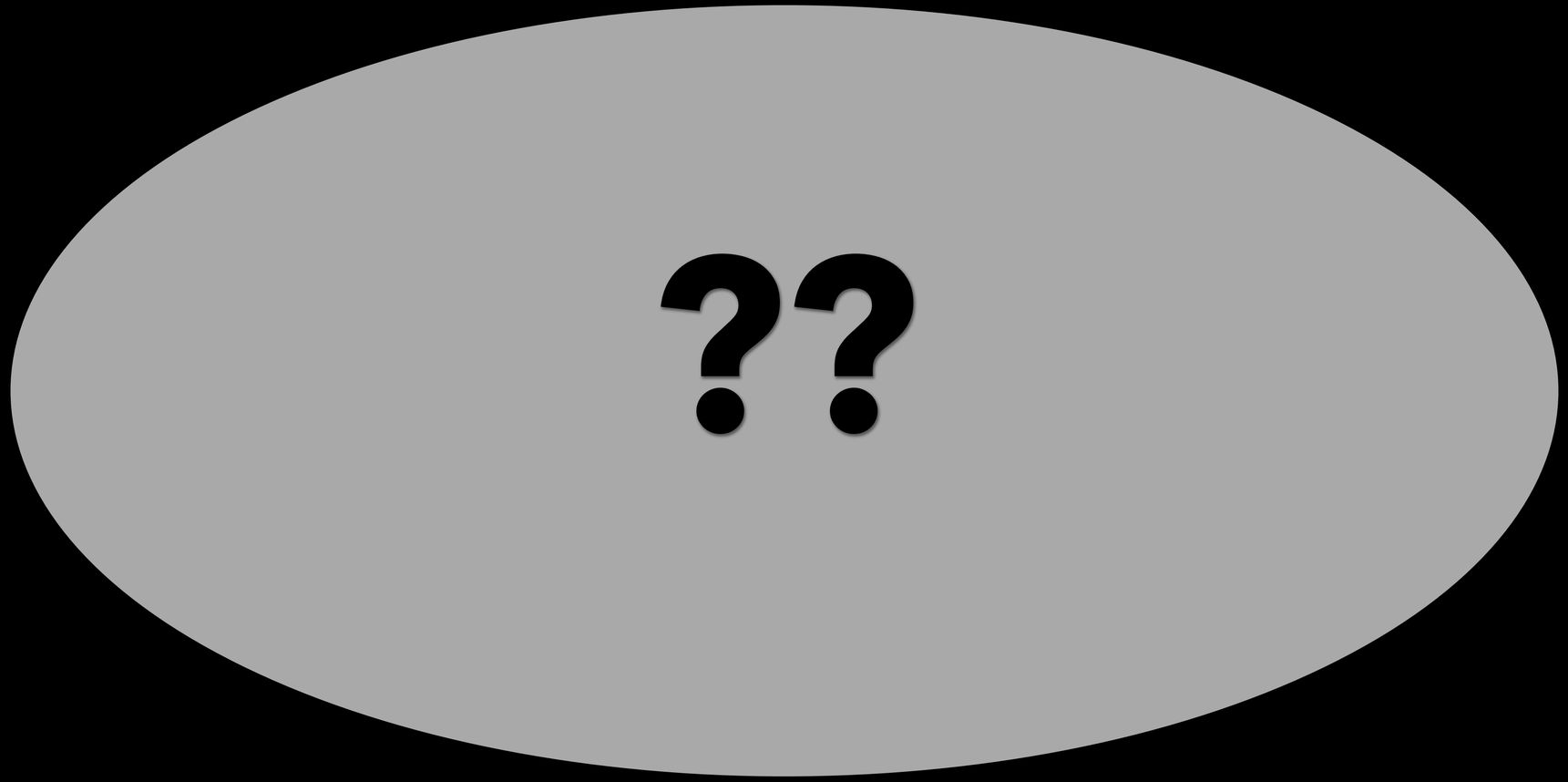

HOW DO WE MAP THE SGWB SKY?

Cross-correlation is essentially
a one-dimensional map of the sky

SGWB MAPPING

Cross-correlation is essentially a one-dimensional map of the sky.

When we consider the time delay between two detectors and the Rotation of the earth.

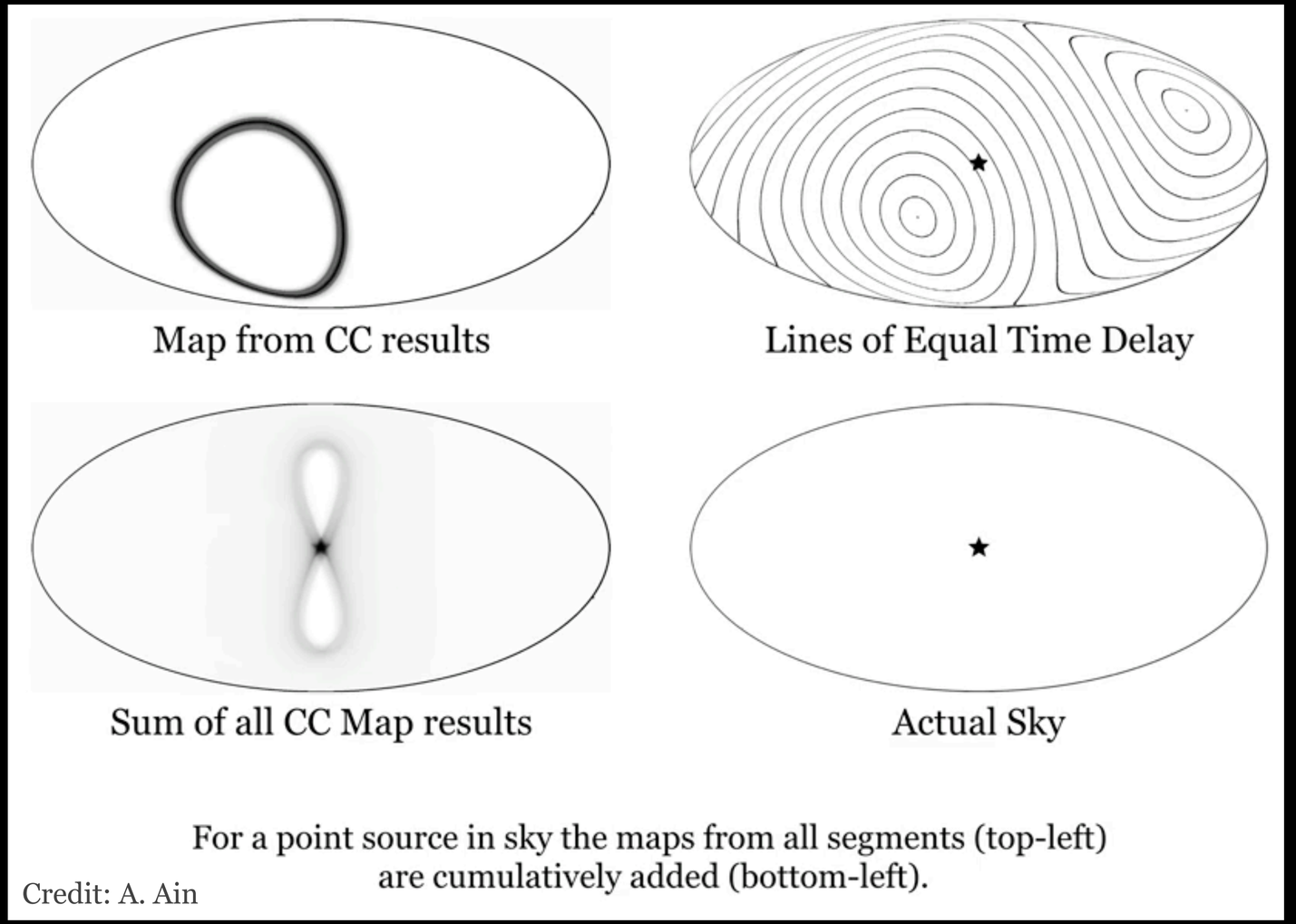

For a point source in sky the maps from all segments (top-left) are cumulatively added (bottom-left).

Credit: A. Ain

- LIGO Hanford-Livingston baseline.
- Assume that the detector has perfect sky coverage.
- No detector noise.
- Strong monochromatic signal.

SGWB MAPPING

Cross-correlation is essentially a one-dimensional map of the sky.

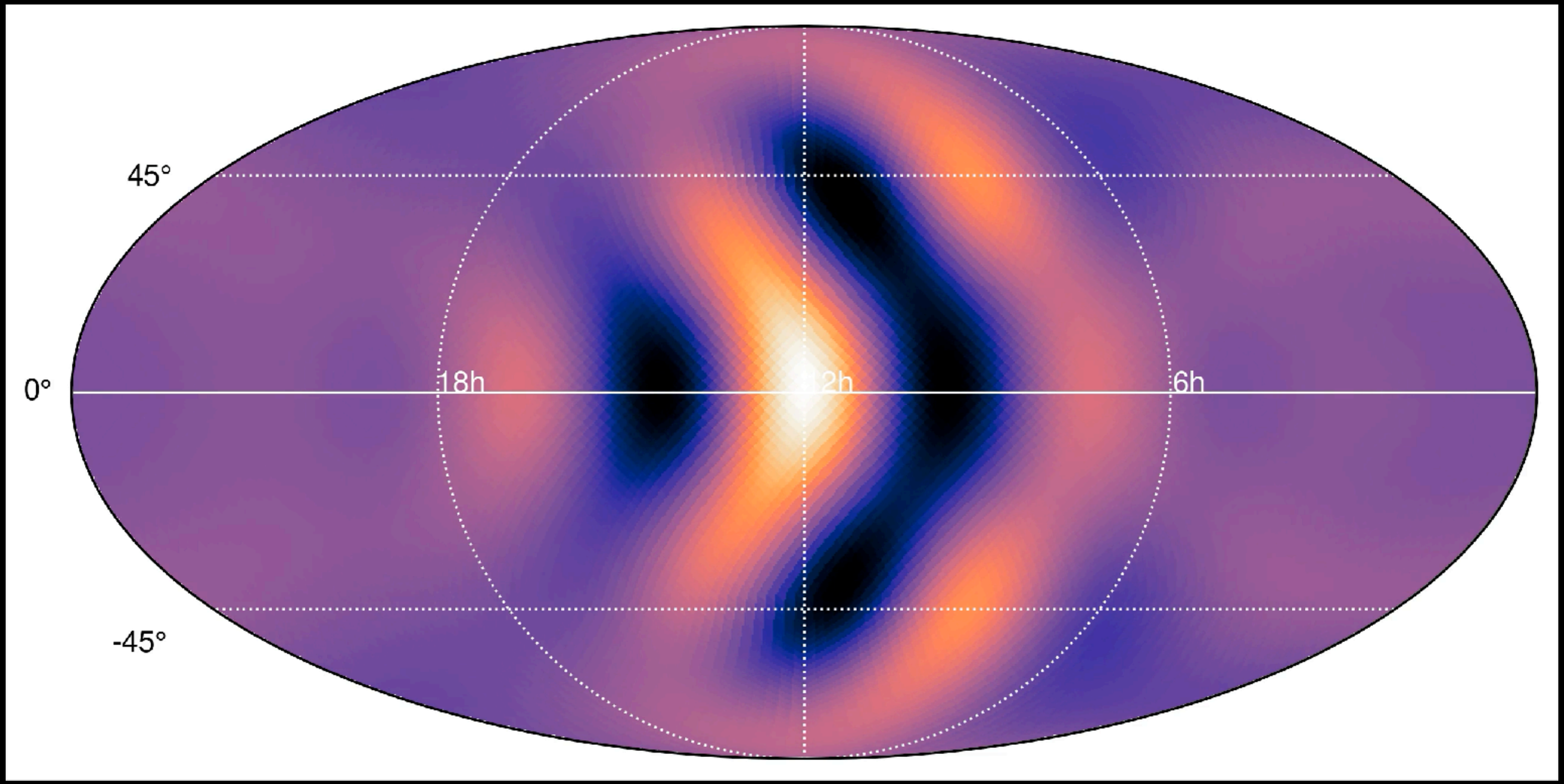

- LIGO Hanford-Livingston baseline.
- Consider the actual antenna pattern.
- Assume O3 detector noise.
- Strong monochromatic signal.

ANISOTROPIC SEARCH

Anisotropic search tries to measure the direction of the sky from where the signal comes.
In this mapping process, we consider:

- The time delay between two detectors
- Rotation of the earth.

SGWB energy density $\Omega_{\rm gw}(f,\hat{\mathbf{n}}) \equiv \frac{f}{\rho_c}\frac{d\rho_{\rm GW}}{df} = \frac{2\pi^2}{3H_0^2} f^3 \mathscr{P}(f,\hat{\mathbf{n}})$

Cross-correlation is essentially a one-dimensional map of the sky.

Anisotropy can be expanded in pixel or spherical harmonic basis

$$\mathscr{P}(f,\hat{\mathbf{n}}) = \sum_p \mathscr{P}_p(f)\, e_p(\hat{\mathbf{n}})$$

HOW DO WE MAP THE SGWB SKY?

The anisotropy of the SGWB can be characterized using the dimensional energy density parameter

$$\Omega_{\mathrm{gw}}(f,\hat{\mathbf{n}}) \equiv \frac{f}{\rho_c}\frac{d\rho_{\mathrm{GW}}}{df} = \frac{2\pi^2}{3H_0^2} f^3 \mathscr{P}(f,\hat{\mathbf{n}})$$

Most of the analysis performed so far assumes that the frequency and direction dependence can be separated: $\mathscr{P}(f,\hat{\mathbf{n}}) = P(\hat{\mathbf{n}})\,H(f)$

Where the common choic[illegible] spectral shape is $H(f) = \left(\frac{f}{f_{\mathrm{ref}}}\right)^{\beta}$

We will perform a model-independent search

ANISOTROPIC SEARCH

To measure the anisotropy $\mathscr{P}(f, \hat{\mathbf{n}})$, the radiometer method uses the maximum likelihood estimator as the statistics

$$\mathscr{P}(f, \hat{\mathbf{n}}) = \Gamma^{-1}_{nn'}(f)\, X_n(f)$$

Dirty Map –> Map of the SGWB convolved with the detector's response.

Clean Map –>Deconvolved map

Fisher Matrix –> Covariance matrix of the dirty map.

Dirty map

$$X_n(f) \propto \sum_t \frac{\gamma^*_{ft,n}\, C(t;f)}{P_1(t;f)\, P_2(t;f)}$$

Fisher information matrix

$$\Gamma_{nn'}(f) \propto \sum_t \frac{\gamma^*_{ft,n}\, \gamma_{ft,n}}{P_1(t;f)\, P_2(t;f)}$$

OVERLAP REDUCTION FUNCTION

To measure the anisotropy $\mathcal{P}(f,\hat{\mathbf{n}})$, the radiometer method uses the maximum likelihood estimator as the statistics

$$\mathcal{P}(f,\hat{\mathbf{n}}) = \Gamma^{-1}_{nn'}(f)\, X_n(f)$$

Recall from Joe's talk:

The overlap function encodes the reduction in sensitivity of a cross-correlation analysis due to separation and misalignment of the detectors.

$$\gamma_{ft,n} :\equiv \sum_A F_1^A(\hat{n},t)\, F_2^A(\hat{n},t)\, e^{2\pi i f\, \hat{n}\cdot\Delta x(t)/c}$$

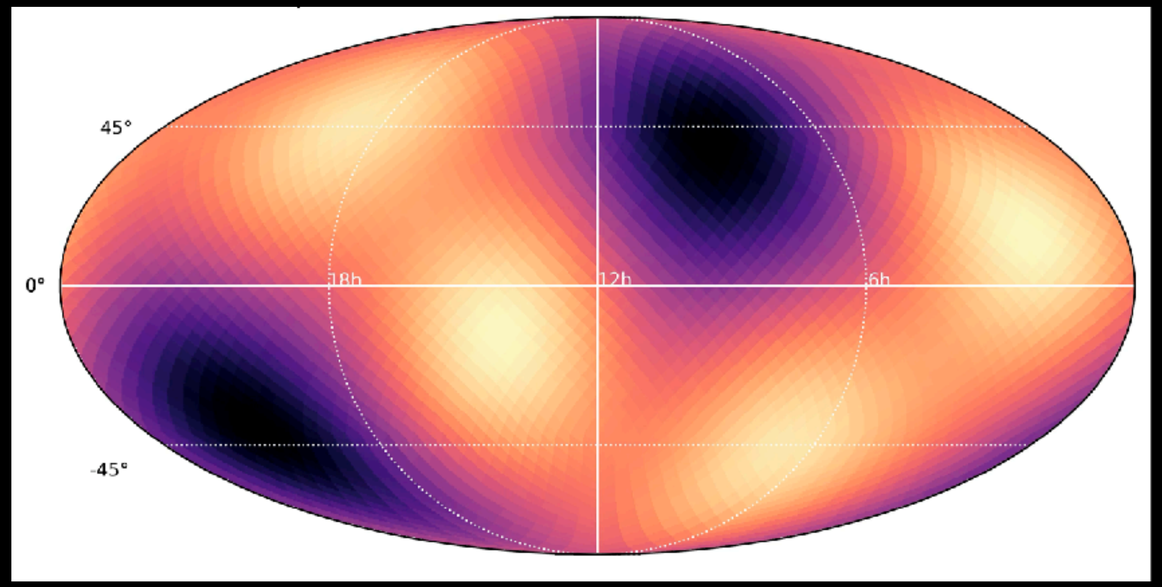

combined antenna pattern

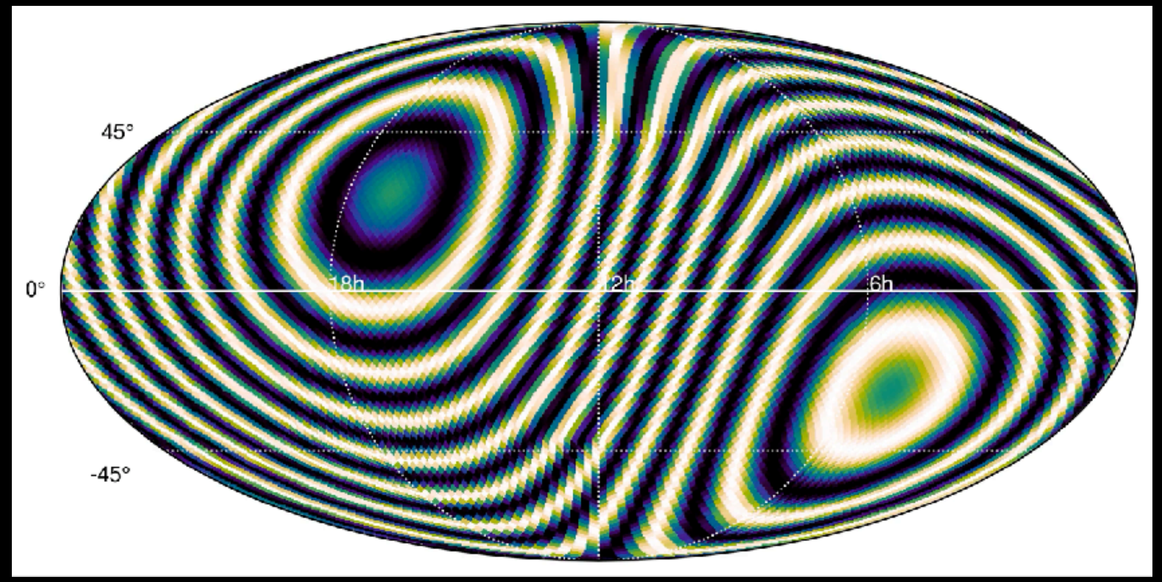

time-delay

OVERLAP REDUCTION FUNCTION

To measure the anisotropy $\mathcal{P}(f, \hat{\mathbf{n}})$, the radiometer method uses the maximum likelihood estimator as the statistics

$$\mathcal{P}(f, \hat{\mathbf{n}}) = \Gamma^{-1}_{nn'}(f)\, X_n(f)$$

Recall:

The overlap function encodes the reduction in sensitivity of a cross-correlation analysis due to separation and misalignment of the detectors.

$$\gamma_{ft,n} :\equiv \sum_A F_1^A(\hat{n}, t)\, F_2^A(\hat{n}, t)\, e^{2\pi i f\ \hat{n}\cdot\Delta x(t)\ /c}$$

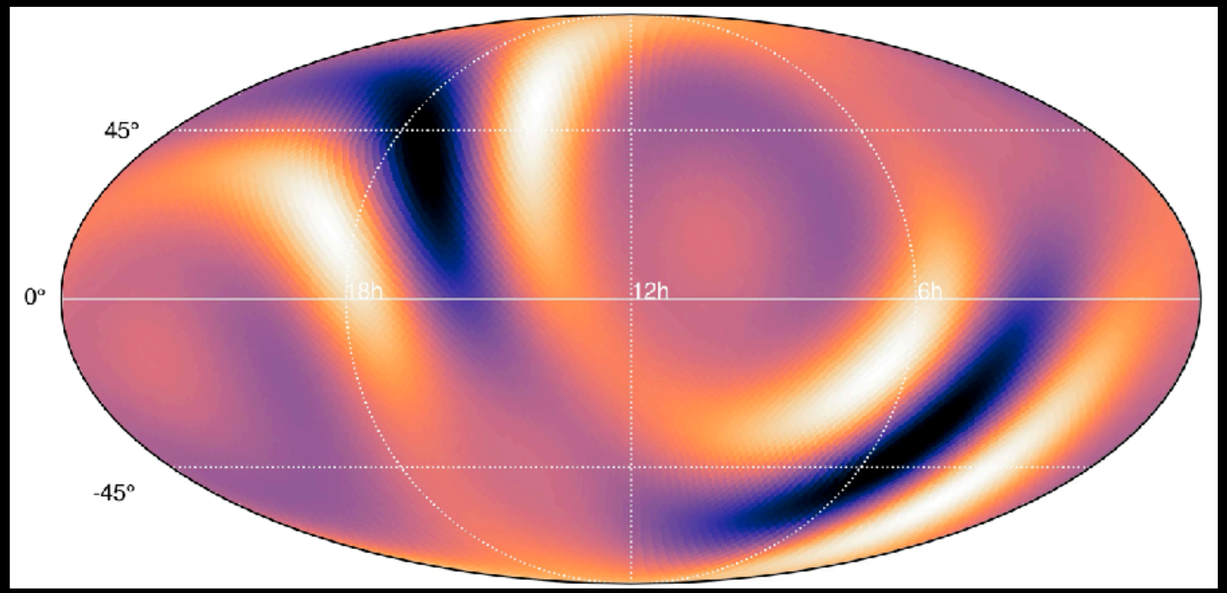

$\gamma_{t,n}\big|_{f=100\text{Hz}}$

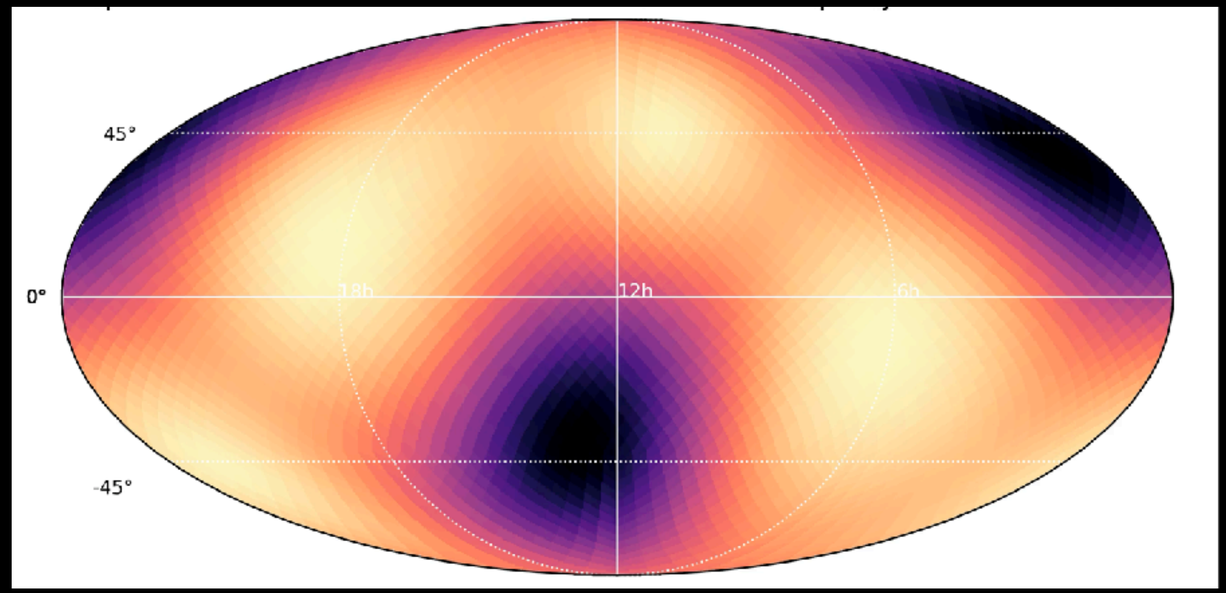

$\gamma_{f,n}\big|_{t=1326542418}$

ANISOTROPIC SEARCH

To measure the anisotropy $\mathscr{P}(f, \hat{\mathbf{n}})$, the radiometer method uses the maximum likelihood estimator as the statistics

$$\mathscr{P}(f, \hat{\mathbf{n}}) = \Gamma^{-1}_{nn'}(f)\, X_n(f)$$

Dirty map

$$X_n(f) \propto \sum_t \frac{\gamma^*_{ft,n}\, C(t;f)}{P_1(t;f)\, P_2(t;f)}$$

Fisher information matrix

$$\Gamma_{nn'}(f) \propto \sum_t \frac{\gamma^*_{ft,n}\, \gamma_{ft,n}}{P_1(t;f)\, P_2(t;f)}$$

DATA PROCESSING

- Time-series data are sampled at 16384 Hz.
    - Downsample to 4096 Hz, so Nyquist frequency is 2048 Hz.
    - Analyze data below 1726 Hz to avoid aliasing effects.
- The high-pass filter is applied to remove the low-frequency noise
- Divide data into time segments of duration T=192 seconds (Hann-windowed and overlapped by 50%).
- Compute discrete Fourier transform on each segment and coarse-grain the spectrum 1/32 Hz.
- Time-domain (stationary cut) and Frequency-domain data cuts.

DataSet

$\tau = 192$ second —> segment duration

$f_{\text{min}} = 20\,\text{Hz}, f_{\text{max}} = 1726\,\text{Hz}$ —> frequency range

$\Delta f = 1/32$ —> Frequency resolution

DATA FOLDING

Ain+ PRD 92, 022003 (2015)

Folding stochastic data to one sidereal day

No approximation, based on a mathematical symmetry

Incorporates all the dirty stuff (quality cuts, overlapping window correction)

Since we are applying earth rotation synthesis imaging, the GW radiometer algebra has a period of one sidereal.

Both dirty map and Fisher matrix computation involve summations over time segments marked by t.

These summations can be split into two parts: $t = i_{\text{day}} \times T_s + t_s$

integer representing the sidereal day number, where t lies

the duration of one sidereal day

remainder within that sidereal day

DATA FOLDING

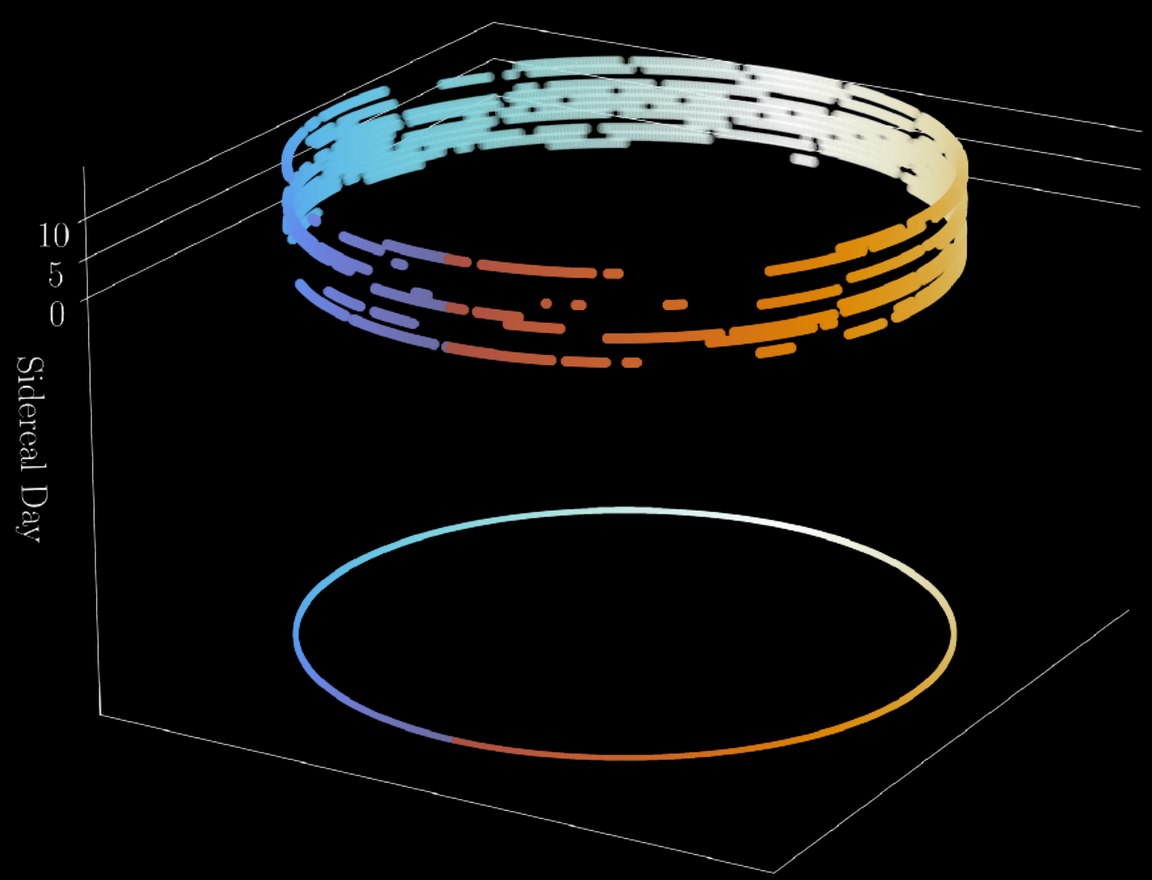

From 10-day data

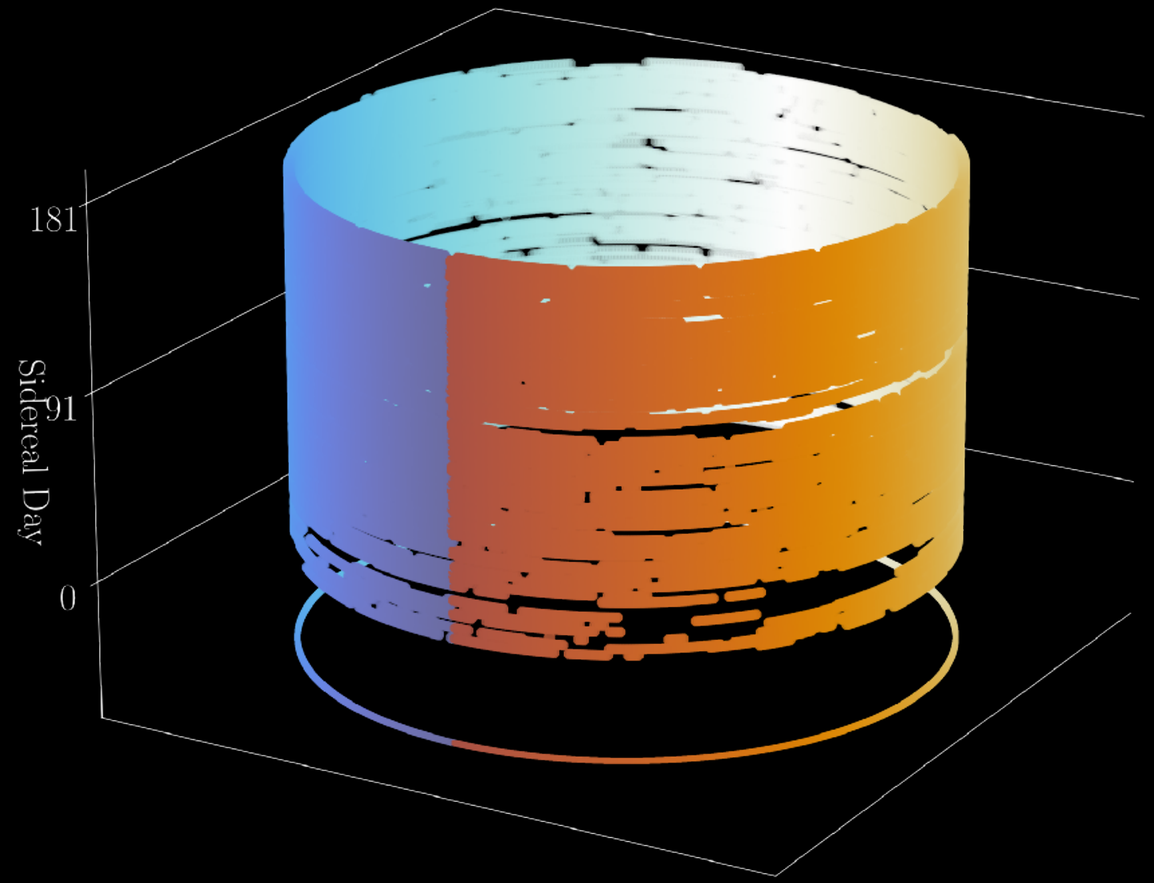

From 6-month data

DATA FOLDING

From O3 ~1 year data

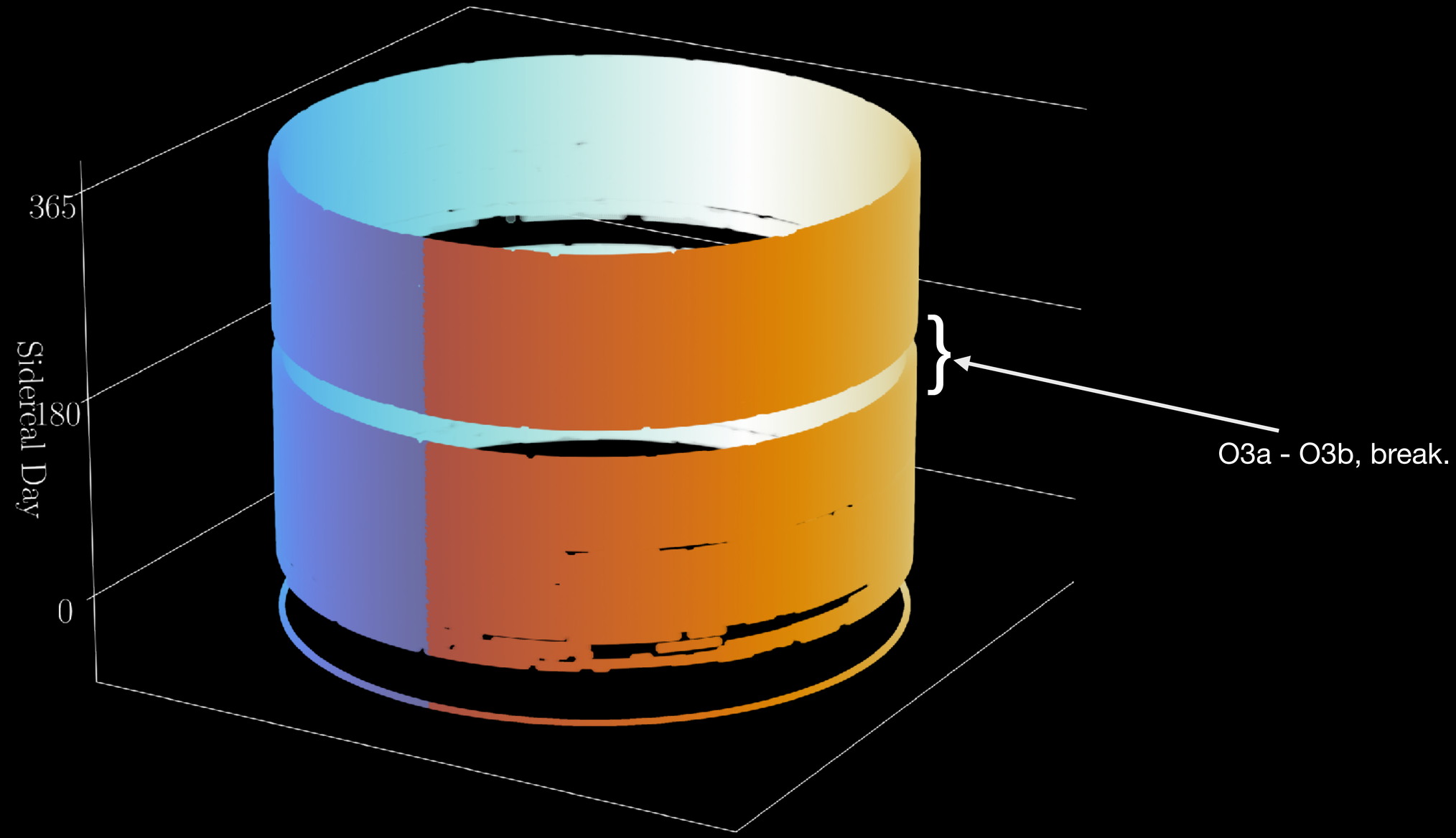

FOLDED DATASET

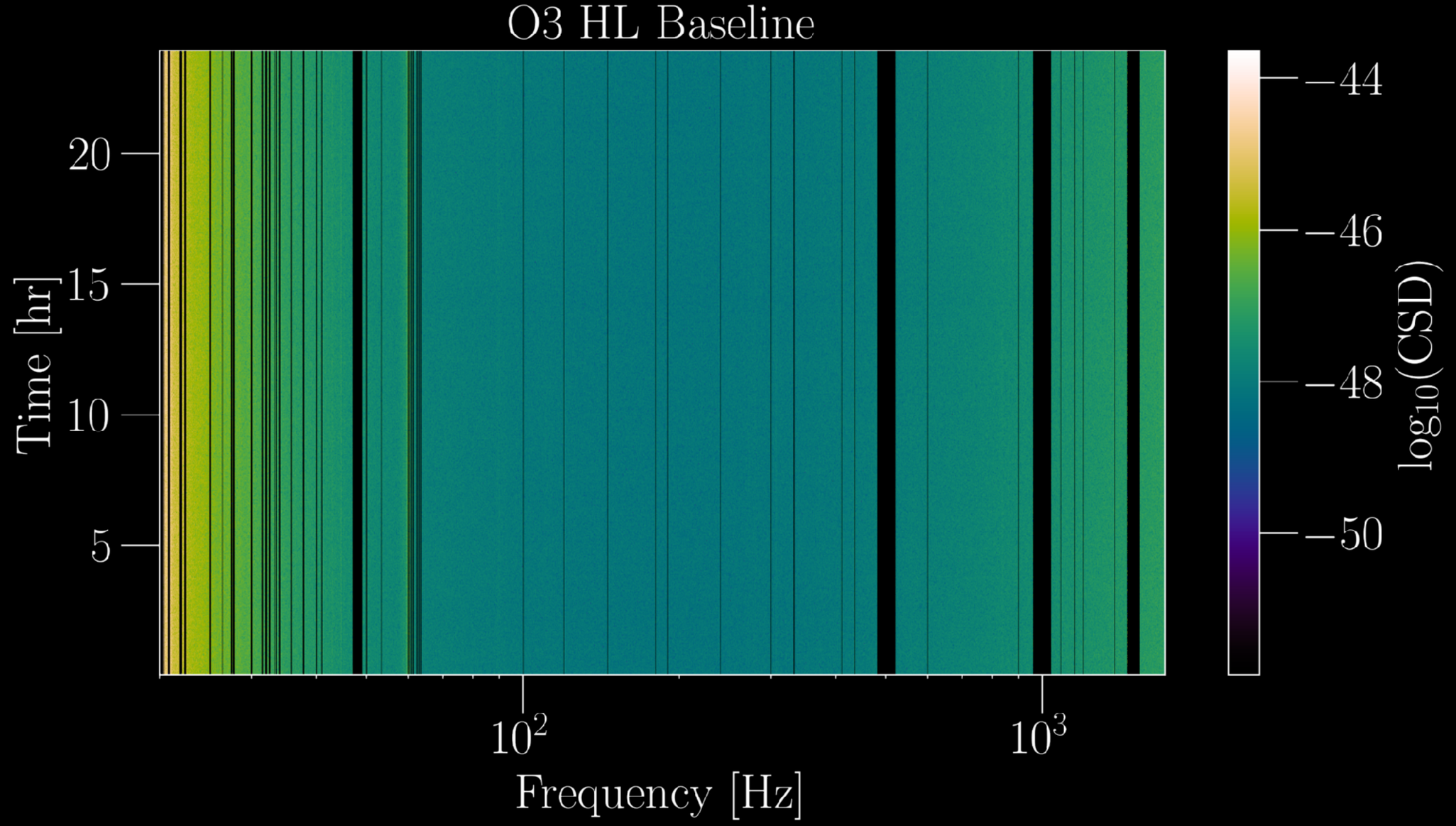

FOLDED DATASET

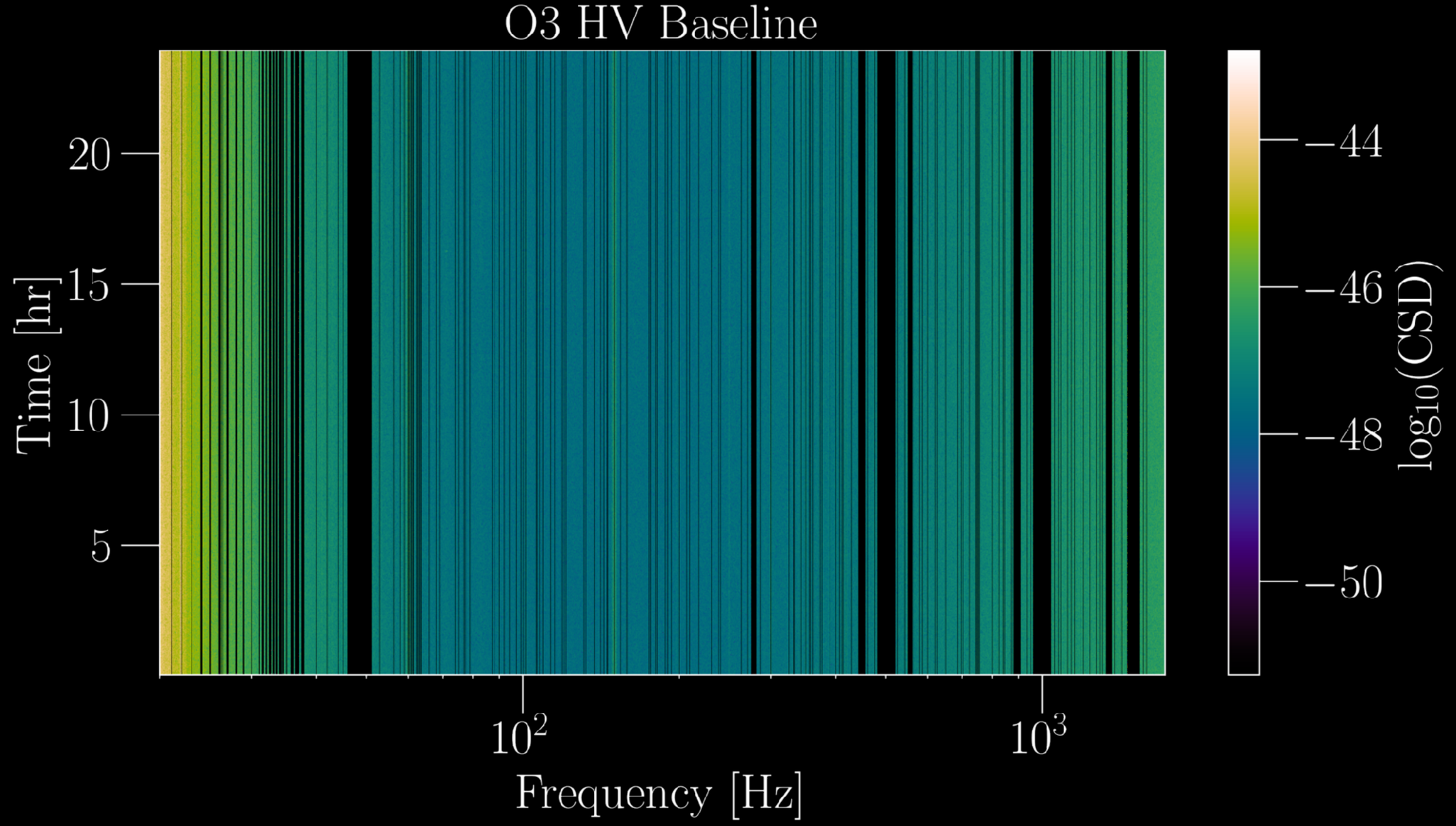

FOLDED DATASET

O1+O2+O3 data set: https://doi.org/10.5281/zenodo.6326656

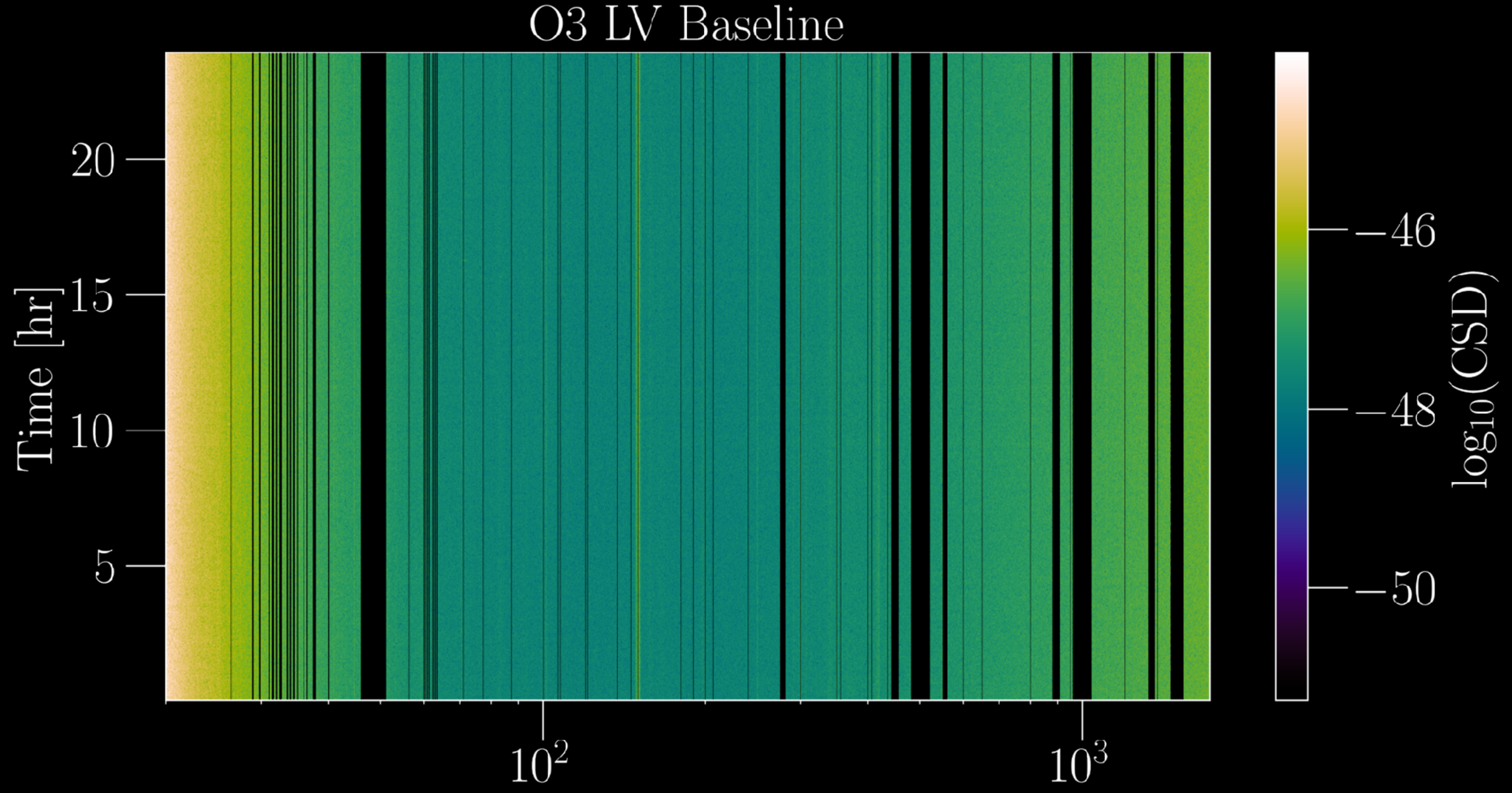

The O1+O2+O3 folded data set can be found at:
https://doi.org/10.5281/zenodo.6326656

PyStoch: MAP-MAKING PIPELINE

Ain, Suresh, Mitra PRD 98, 024001 (2018)
Suresh, Ain, Mitra PRD 103, 083024 (2021)

PyStoch : fast HEALPix based SGWB mapmaking

↓

perform the whole analysis on a laptop in less than an hour*

↓

Produces the narrowband maps as an intermediate result

so separate search for different frequency spectra becomes redundant

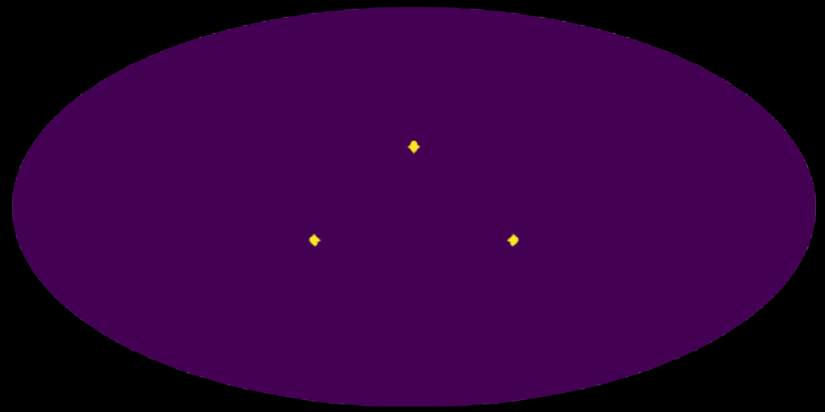

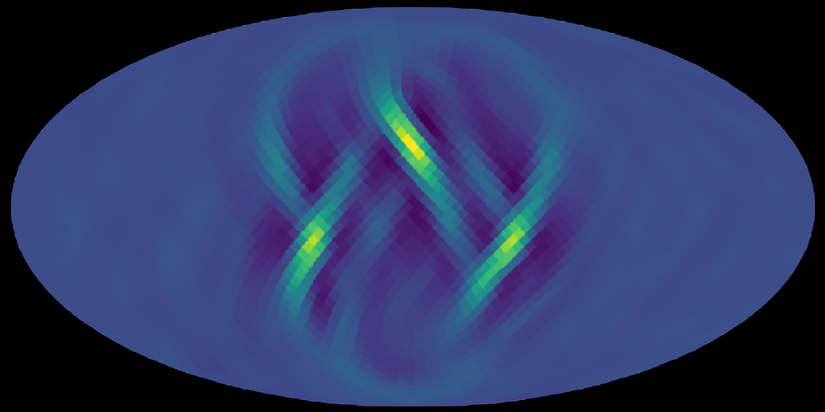

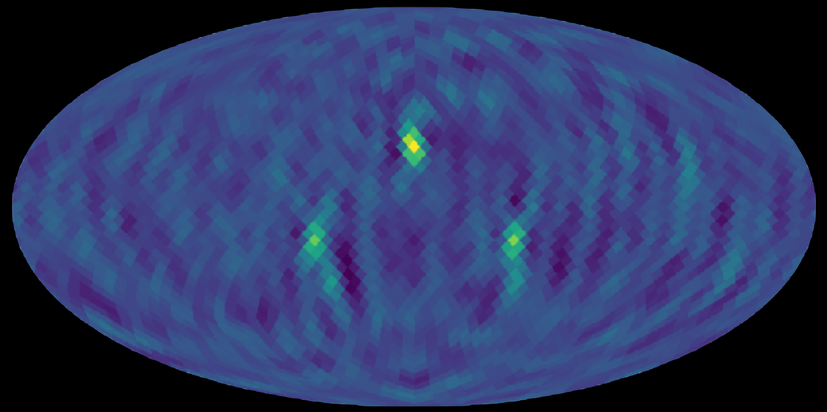

* We have used sidereally folded data (PRD 92, 022003 2015) set for this analysis

https://git.ligo.org/stochastic-public/stochastic.git

ALL-SKY ALL-FREQUENCY SEARCH

Now we have all the ingredients to perform an all-sky, all-frequency search, which assumes **no** specific power-law model for the SGWB

20 Hz

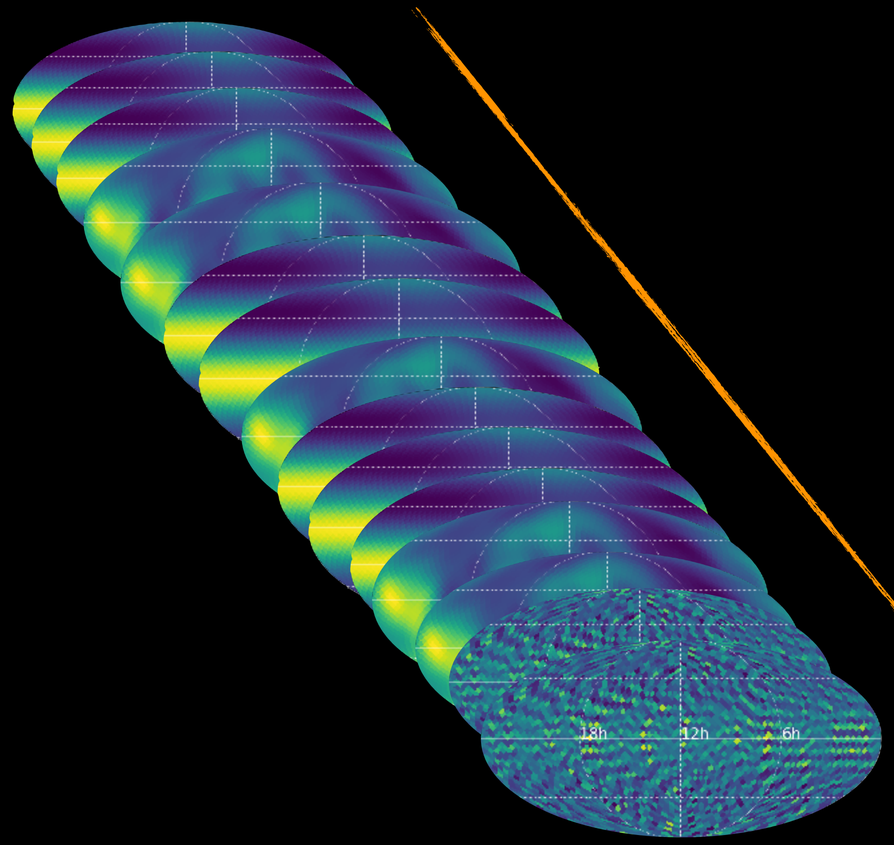

SGWB sky maps at every frequency bins

~1500 Hz

ALL-SKY ALL-FREQUENCY SEARCH

Now we have all the ingredients to perform an all-sky, all-frequency search, which assumes **no** specific power-law model for the SGWB

We presented the **first atlas** of SGWB sky from this analysis.

Phys.Rev.D 105 (2022) 10, 102001

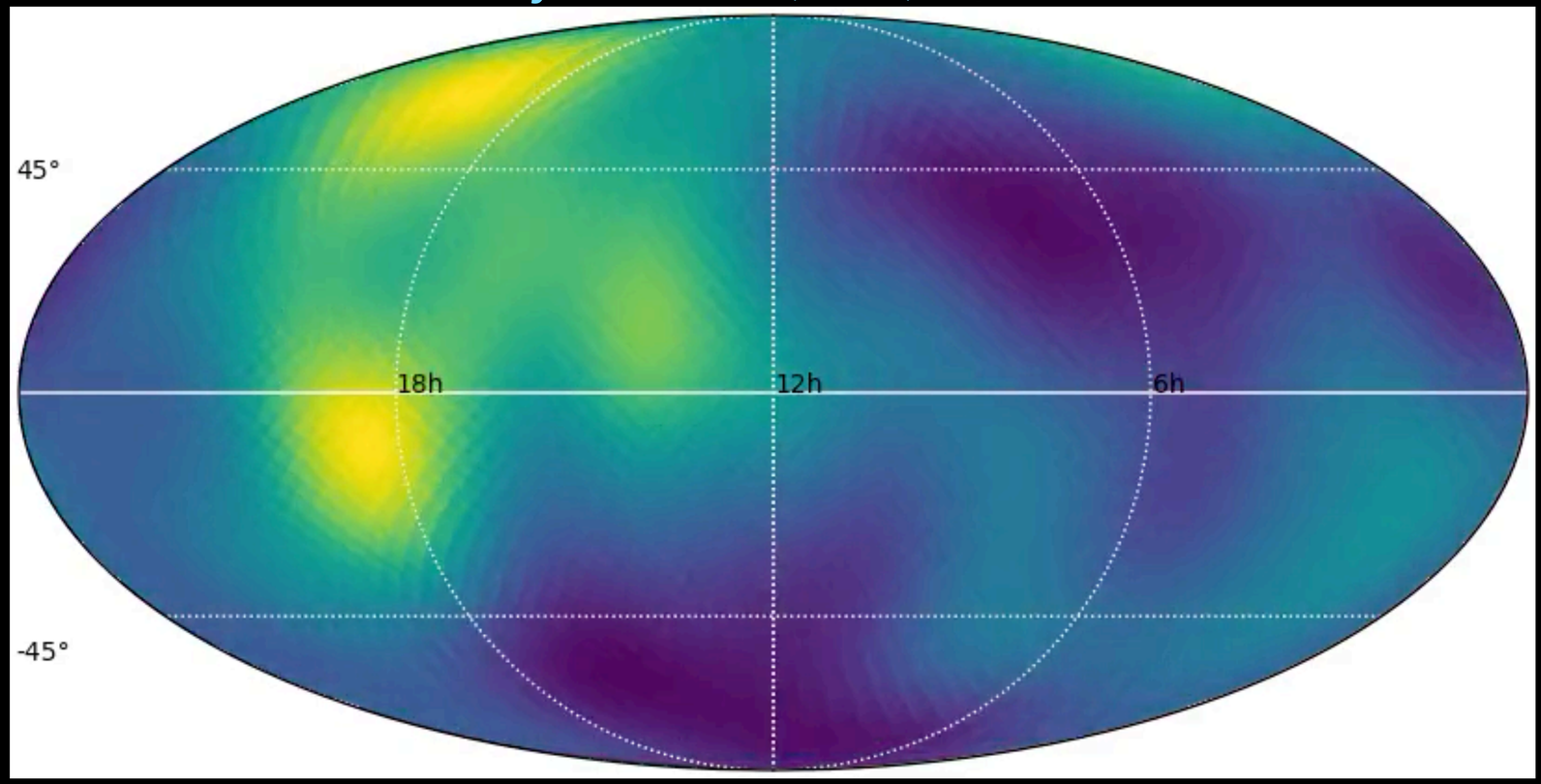

ALL-SKY ALL-FREQUENCY SEARCH

Phys.Rev.D 105 (2022) 10, 102001

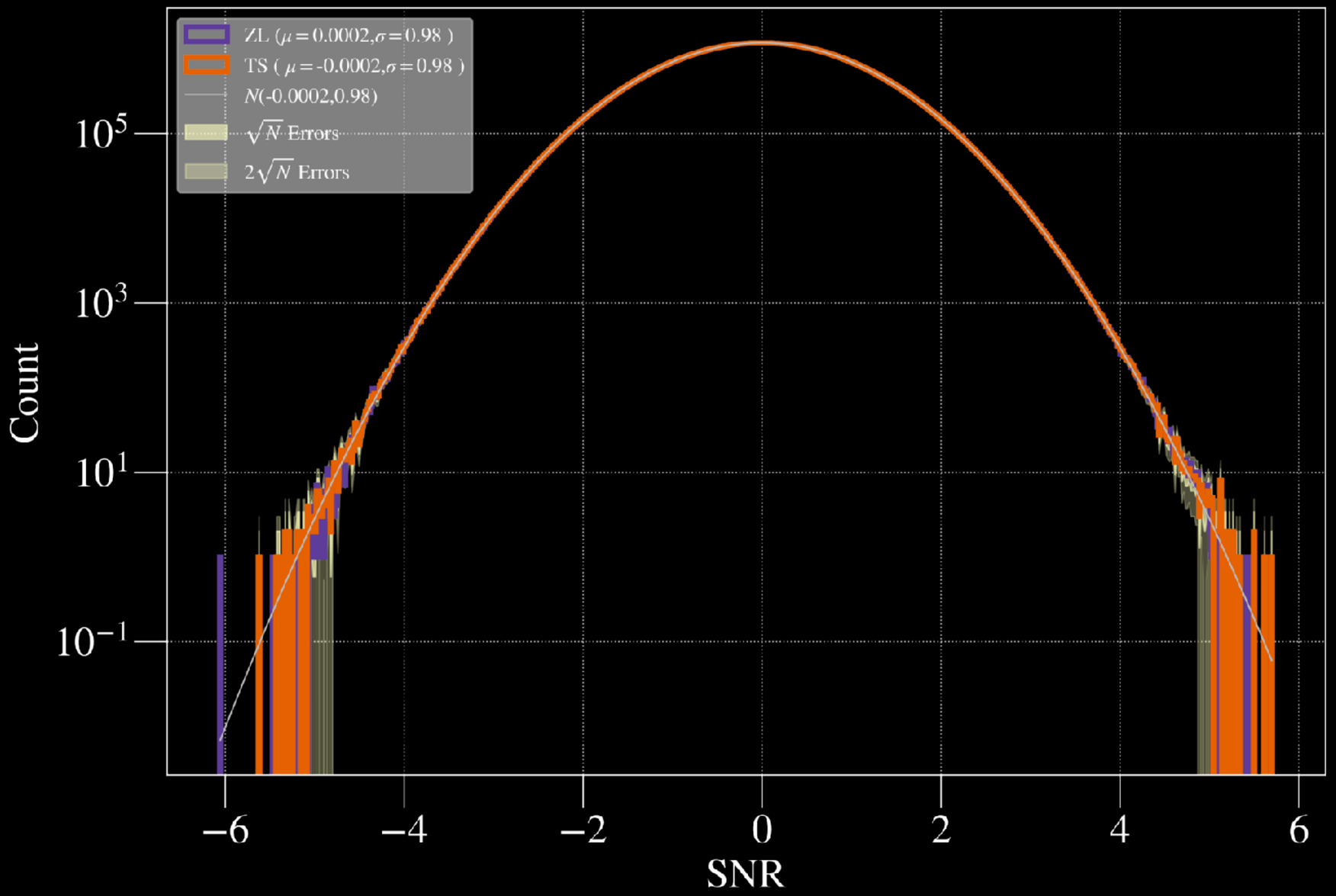

TS –> a random time-shift to each contiguous slice of data such that the net shift (1–2 seconds) is always much greater than the physically permissible time delay.

The zero-lag (ZL) data is consistent with the time-shifted (TS) data within 2-sigma error bars.

We performed follow-up studies on the outlier (SNR <-6) and found no astrophysical-motivated channels. This outlier is also statistically insignificant, given the trial factors corrected p-value >5%

Introducing a constant unphysical time-shift of ~1 second between the data streams from a pair of detectors. These constant time- shifts do not completely cancel out the types of sources that have longer coherence, e.g. Isolated NS.

ALL-SKY ALL-FREQUENCY SEARCH

Phys.Rev.D 105 (2022) 10, 102001

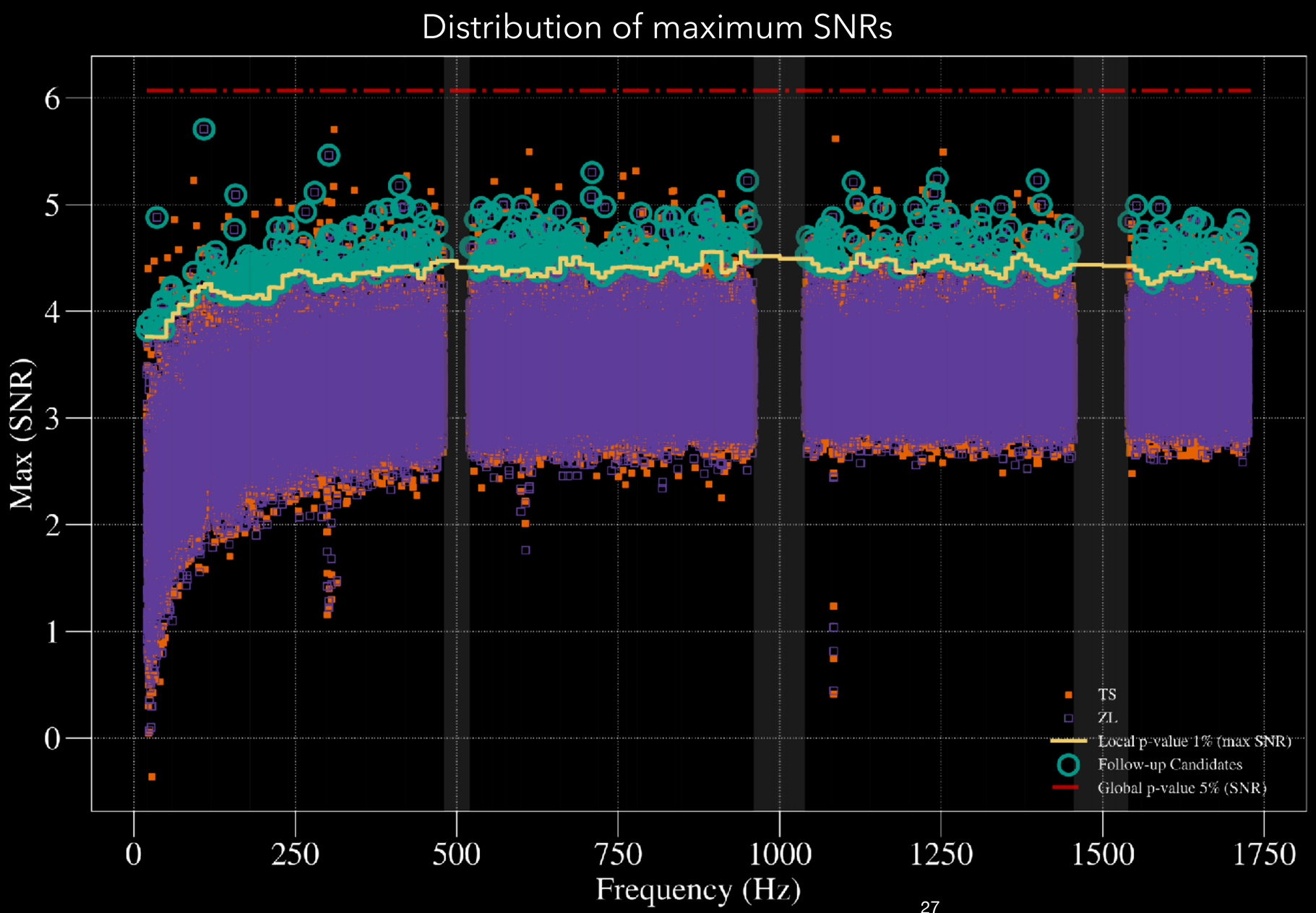

- The yellow curve shows the 99th percentile of maximum SNR for every 10 Hz frequency bin in TS, smoothed over three neighbouring 10 Hz bins.
- The red line delineates the trials-factor-corrected, one-sided global p-value of 5%
- The points above the yellow curve marked with teal circles are the identified candidates for follow-up studies.

ALL-SKY ALL-FREQUENCY SEARCH

Phys.Rev.D 105 (2022) 10, 102001

Given no detection, we set the all-sky all-frequency upper limits on the SGWB effective strain*:

$$h(f, \hat{\mathbf{n}}) = \sqrt{\mathscr{P}(f, \hat{\mathbf{n}})\, df}$$

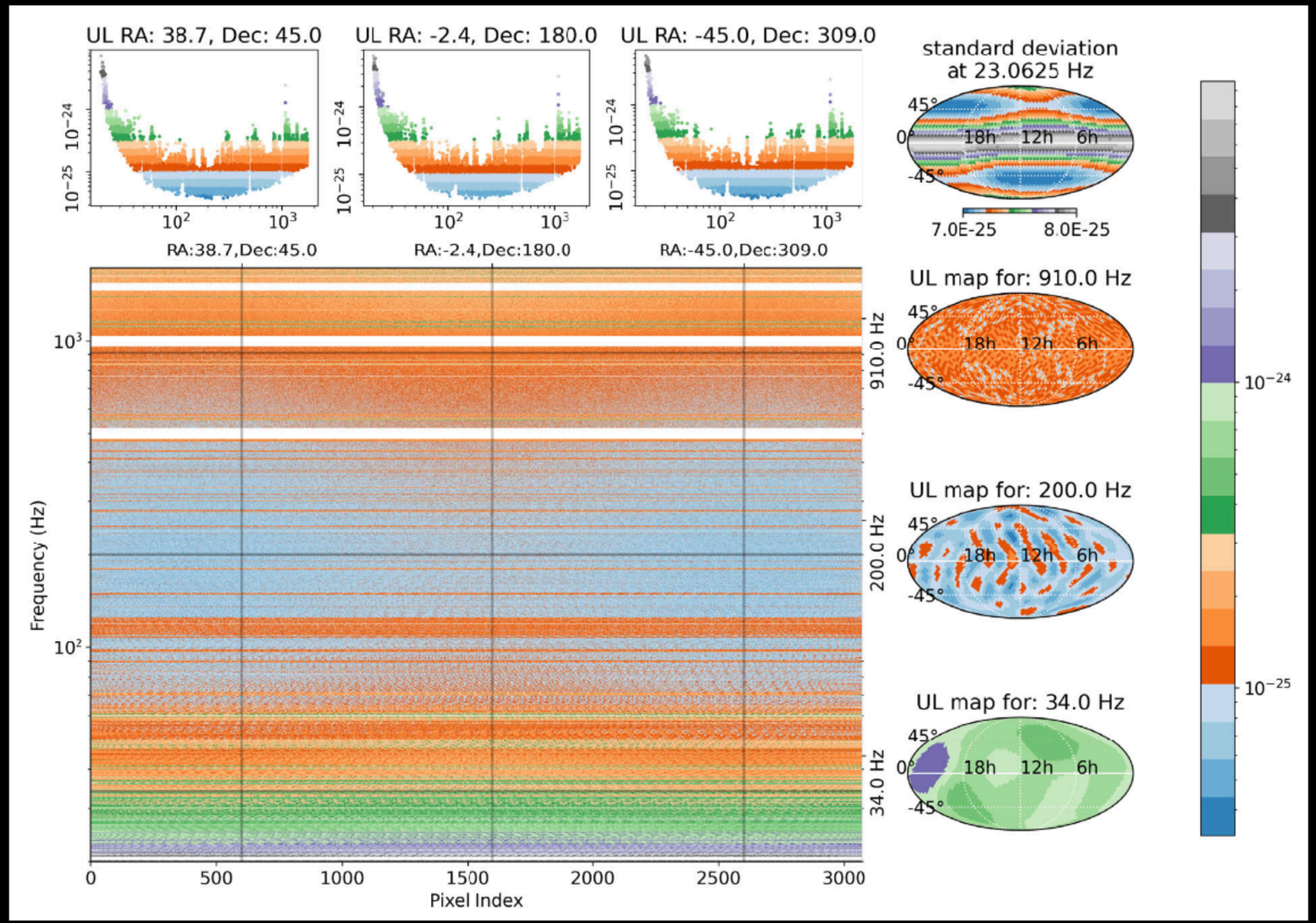

- The colour bar here denotes the range of upper limit variations.
- The vertical cross-section in this diagram shows the frequency-dependent upper limit in a particular direction.
- The Horizontal cross-sections form a map of upper limits in a particular frequency.
- Notched frequencies in a baseline appear as horizontal white bands in the plot.

*circular polarisation without Doppler correction

ALL-SKY ALL-FREQUENCY RESULTS

Phys.Rev.D 105 (2022) 10, 102001

Assume a power law and combine these narrowband maps to obtain the 'usual' broadband results

$$\hat{\mathscr{P}}(\hat{\mathbf{n}}) = \frac{\sum_f \hat{\mathscr{P}}(f,\hat{\mathbf{n}})\,\sigma_{\hat{\mathbf{n}}}^{-2}(f)\,H(f)}{\sum_f \sigma_{\hat{\mathbf{n}}}^{-2}(f)\,H^2(f)}$$

$$\sigma_{\hat{\mathbf{n}}} = \left[\sum_f \sigma_{\hat{\mathbf{n}}}^{-2}(f)\,H^2(f)\right]^{-1/2}$$

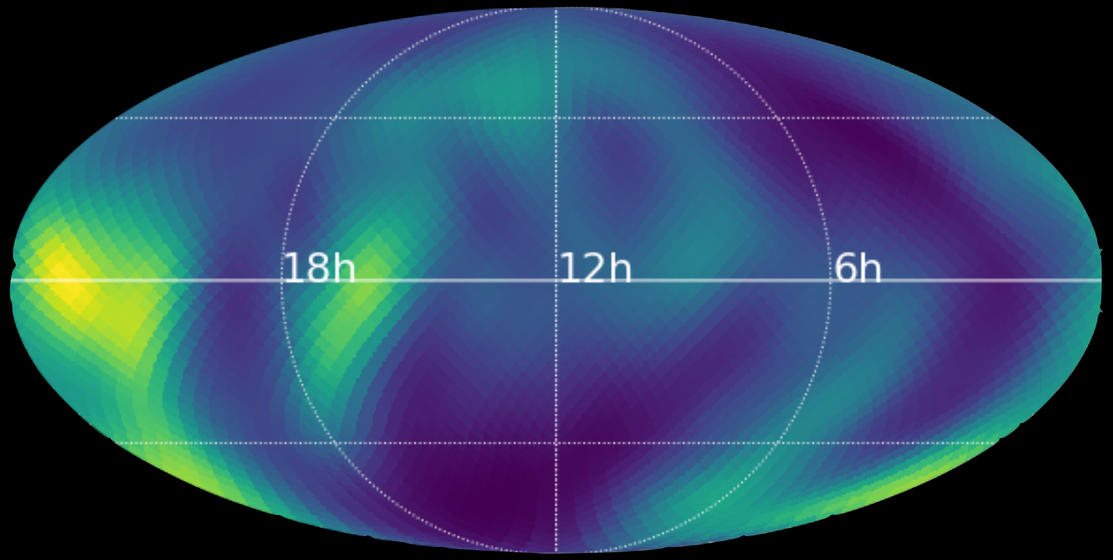

$\alpha = 0$, spectral shape

Assume a power law and sum over all the directions of these narrowband maps to obtain the 'usual' isotropic results

$$\hat{\mathscr{P}}_{\rm iso}(f)\,\sigma_{\rm iso}^{-2}(f) = \frac{5}{4\pi}\int d\hat{\mathbf{n}}\,\hat{\mathscr{P}}(f,\hat{\mathbf{n}})\,\sigma_{\hat{\mathbf{n}}}^{-2}(f)$$

$$\sigma_{\rm iso}^{-2}(f) = \left(\frac{5}{4\pi}\right)^2 \int d\hat{\mathbf{n}} \int d\hat{\mathbf{n}}'\,\Gamma_{\hat{\mathbf{n}},\hat{\mathbf{n}}'}(f)$$

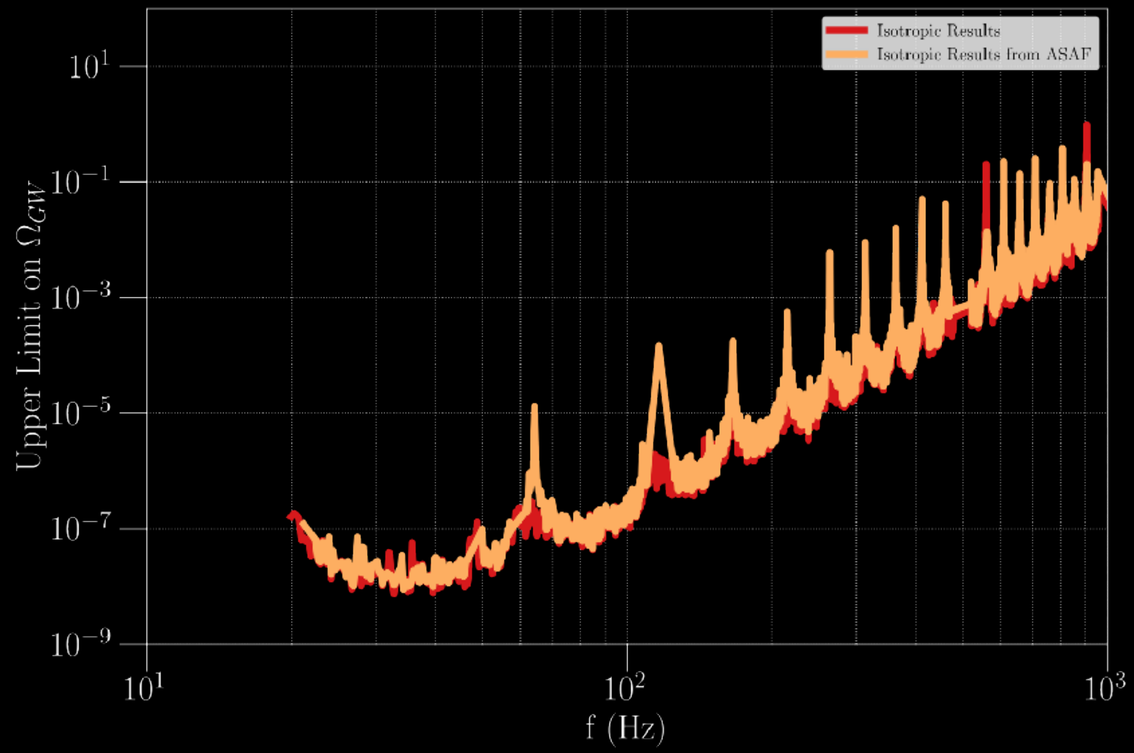

ANGULAR POWER SPECTRA

Suresh+ PRD 103, 083024 (2021)
Agarwal+ PRD 108, 023011 (2023)

Using the SpH basis, it is possible to expand and map the direction–frequency dependent component as

$$\mathscr{P}(f,\hat{n}) = \sum_{lm} \mathscr{P}_{lm}(f) Y_{lm}(\hat{n})$$

The model-independent spherical harmonic coefficients that maximize the likelihood function are given by

$$\mathscr{P}_{lm}(f) = \Gamma^{-1}_{lm,l'm'}(f)\, X_{l'm'}(f)$$

The estimator of the narrowband angular power spectra

$$\hat{C}_{\ell}(f) = \frac{1}{2l+1} \sum_{m} \left[|\hat{\mathscr{P}}_{lm}(f)|^2 - \left[\Gamma^{-1}\right]_{lm,lm}(f) \right]$$

PyStoch is now equipped to perform the above search.

ANGULAR POWER SPECTRA

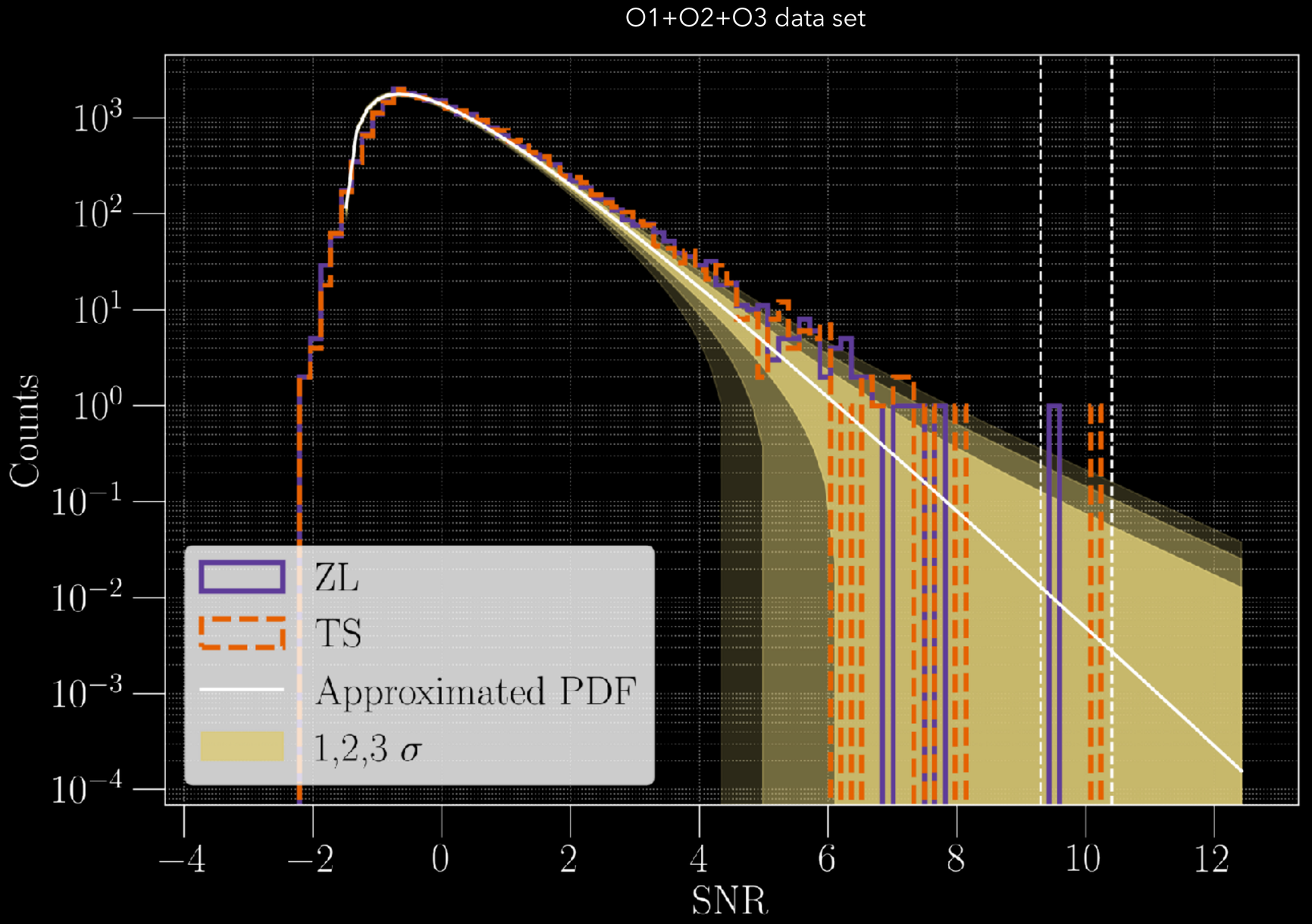

The zero-lag (ZL) data is consistent with the time-shifted (TS) data within 3-sigma error bars.

A few candidates in zero-lag data have SNR above the threshold, which can be due to statistical fluctuations or coupling between the harmonic mode.

ANGULAR POWER SPECTRA

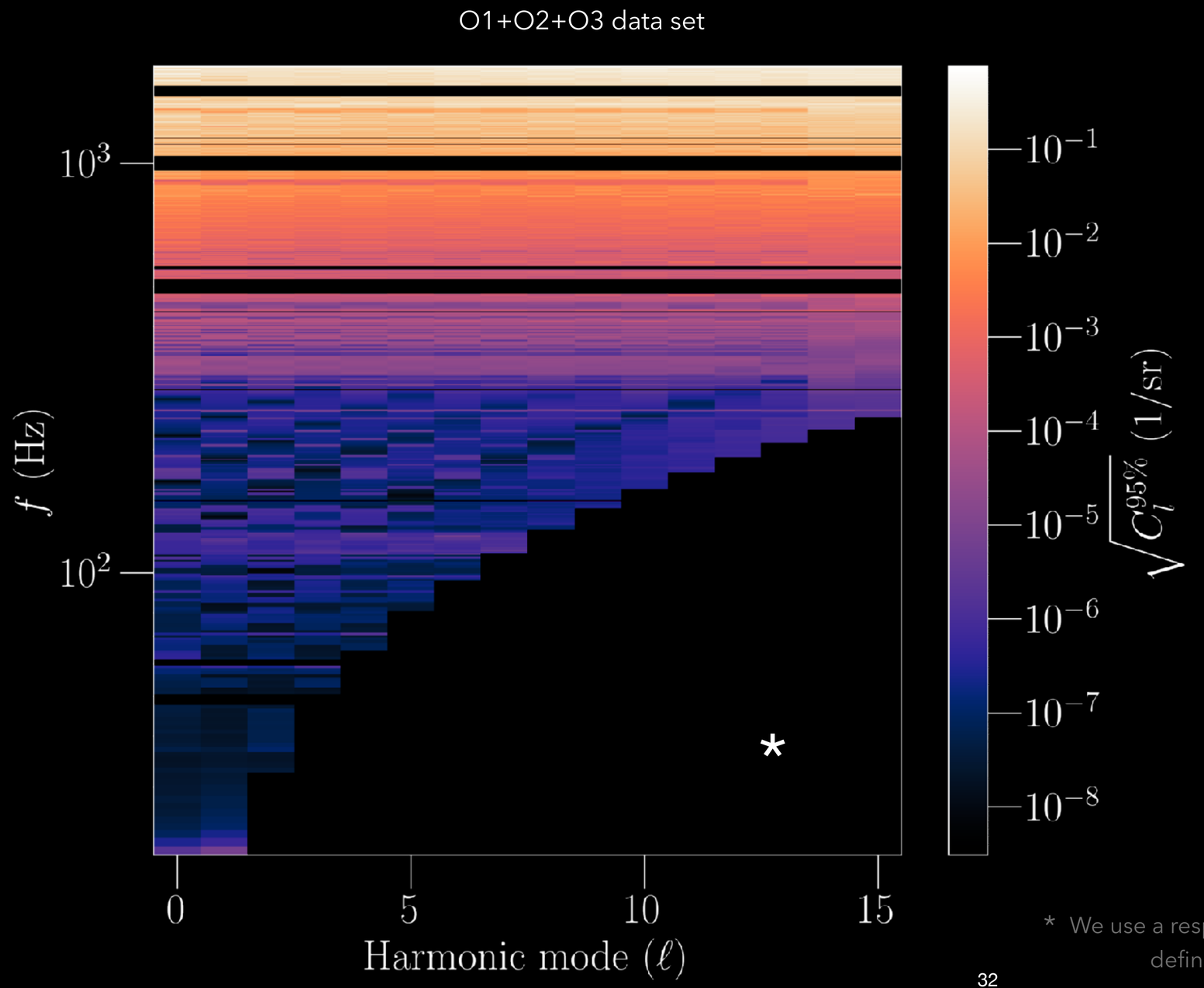

- We can compare different theoretical C_ℓ predictions.
- One can combine these estimates with specific spectral shapes to obtain our 'usual' broadband results.
- Considering the monopole results will yield isotropic results.

See Vuk's talk for the details and its practical applications.

* We use a response matrix to find the suitable angular scale given a frequency. ℓ_{max} is defined as the point where the response falls by 10^{-5} of the maximum.

REAL LIFE COMPLICATIONS

Antenna Pattern Function

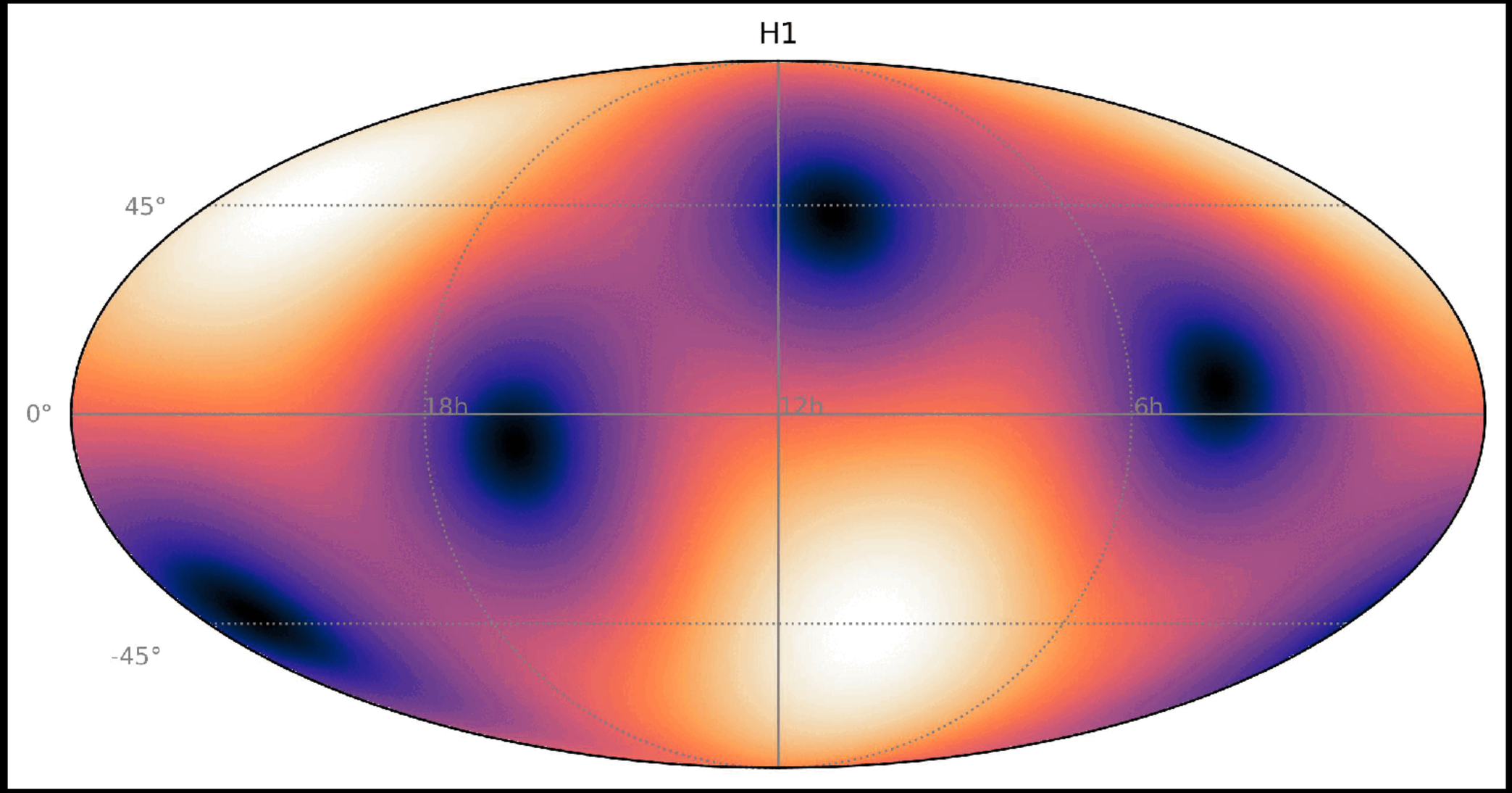

REAL LIFE COMPLICATIONS

Recall:

$$\mathscr{P}(f, \hat{\mathbf{n}}) = \Gamma^{-1}_{nn'}(f)\, X_n(f)$$

$$\Gamma_{nn'}(f) \propto \sum_t \frac{\gamma^*_{ft,n}\, \gamma_{ft,n}}{P_1(t;f)\, P_2(t;f)}$$

Unnormalized $\Gamma_{nn'}$ –> Response function for the pointing direction n. Each column of the beam matrix is a response function

Unnormalized $\Gamma_{nn'}$ –> Point spread function for the source direction n'. Each row of the beam matrix is a point spread function

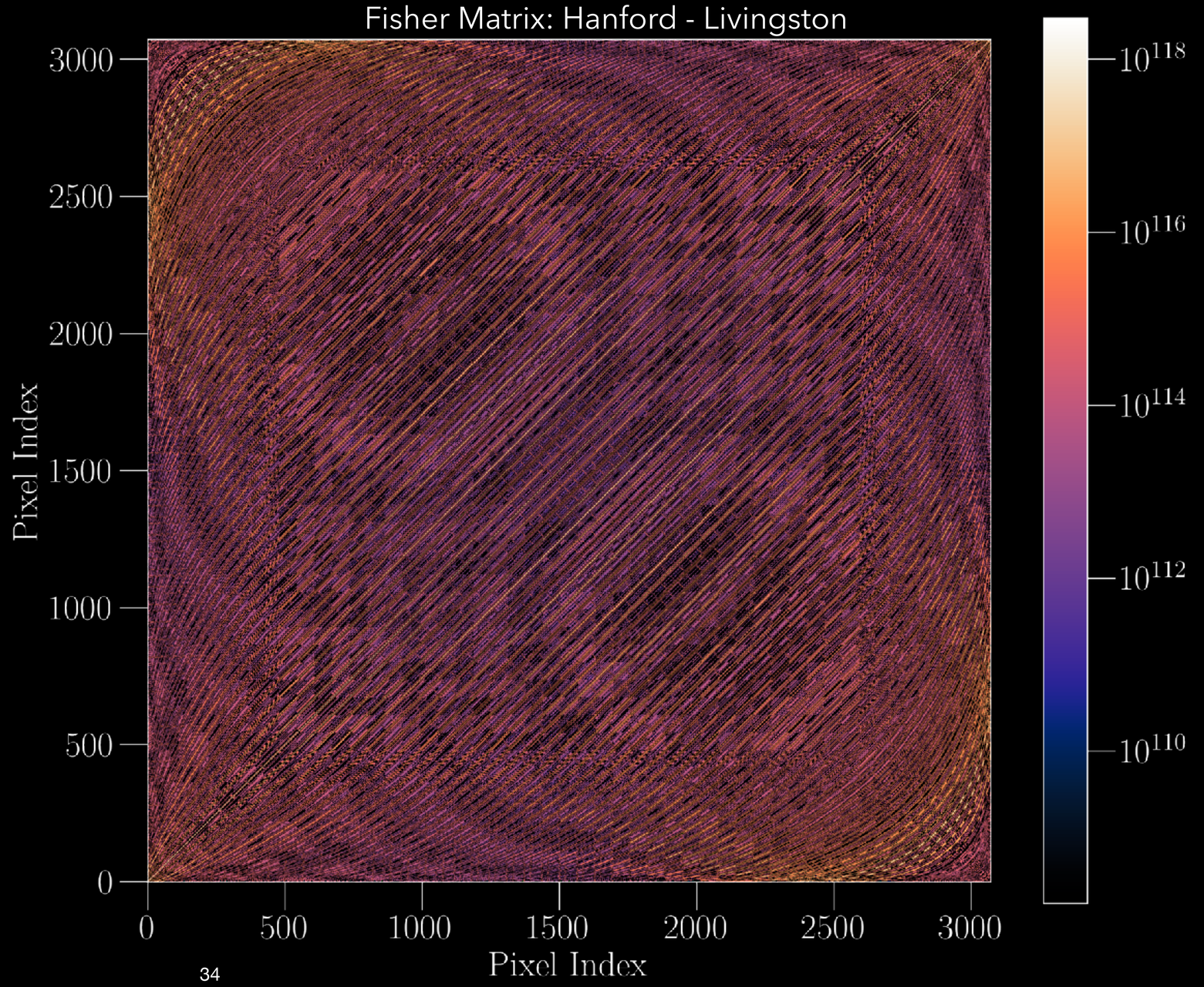

REAL LIFE COMPLICATIONS

Recall:

$$\mathscr{P}(f, \hat{\mathbf{n}}) = \Gamma^{-1}_{nn'}(f)\, X_n(f)$$

$$\Gamma_{nn'}(f) \propto \sum_t \frac{\gamma^*_{ft,n}\, \gamma_{ft,n}}{P_1(t;f)\, P_2(t;f)}$$

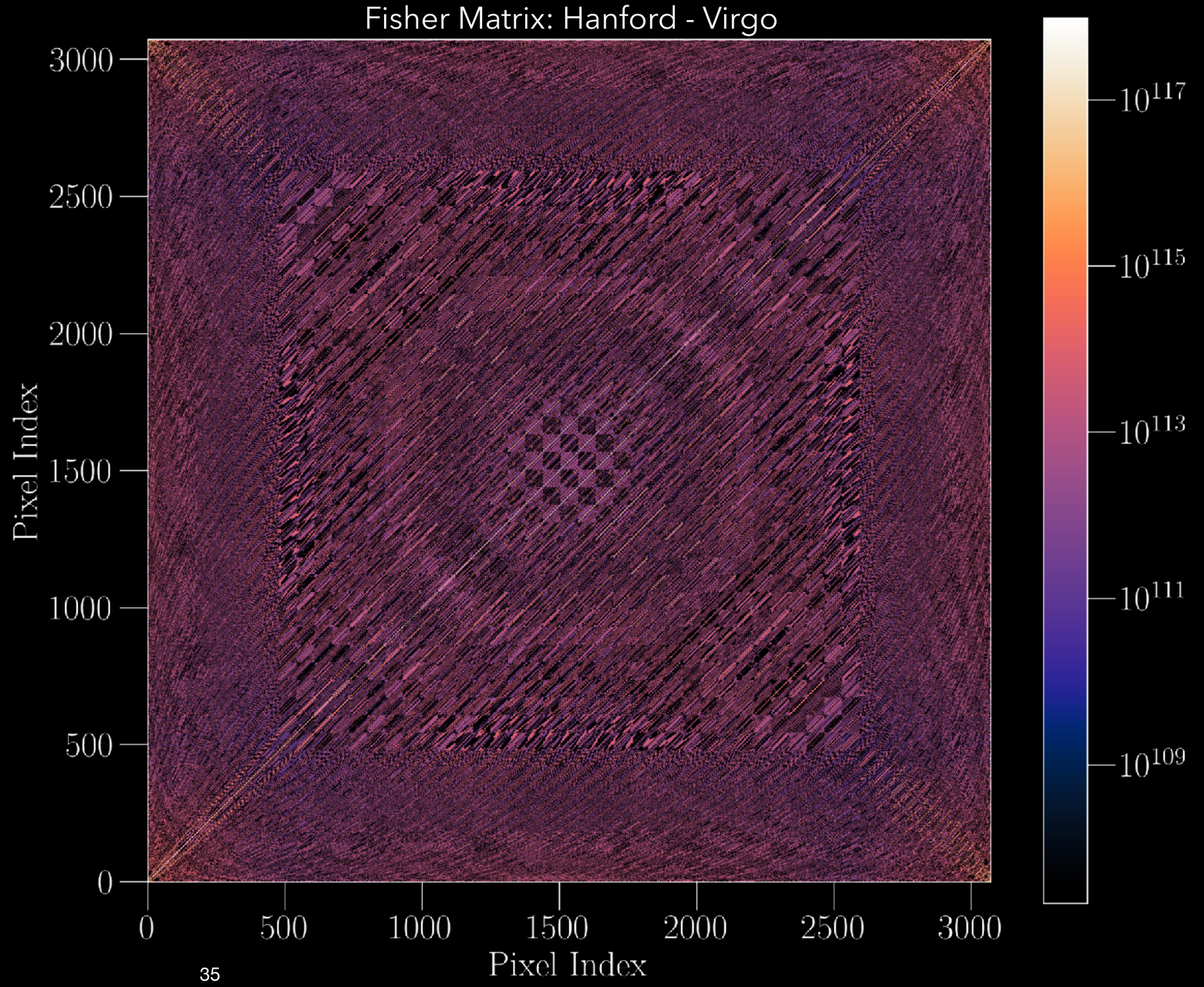

REAL LIFE COMPLICATIONS

Recall:

$$\mathcal{P}(f, \hat{\mathbf{n}}) = \Gamma^{-1}_{nn'}(f)\, X_n(f)$$

$$\Gamma_{nn'}(f) \propto \sum_t \frac{\gamma^*_{ft,n}\, \gamma_{ft,n}}{P_1(t;f)\, P_2(t;f)}$$

CHALLENGE: inverting $\Gamma_{nn'}$

Solutions:
- Regularising the matrix.
- More detectors.

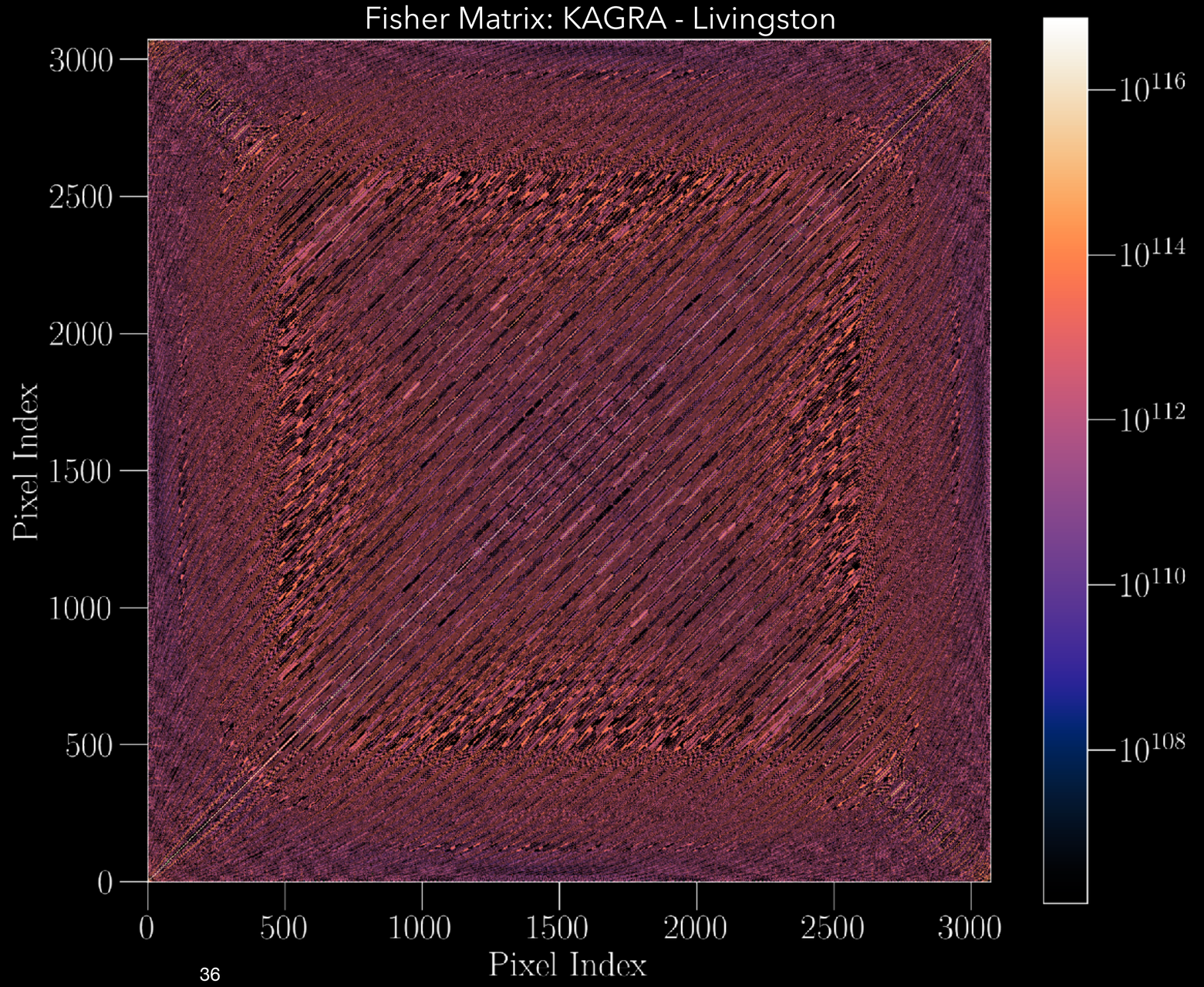

ADDING MORE DETECTORS

$$\Gamma = U S V^{\dagger}$$

U and V are unitary matrices, and S is a diagonal matrix whose nonzero elements are the real and positive eigenvalues of the Fisher matrix, arranged in descending order

Increasing the number of baselines considered in the analysis will act as a natural regulariser for the Fisher Matrix.

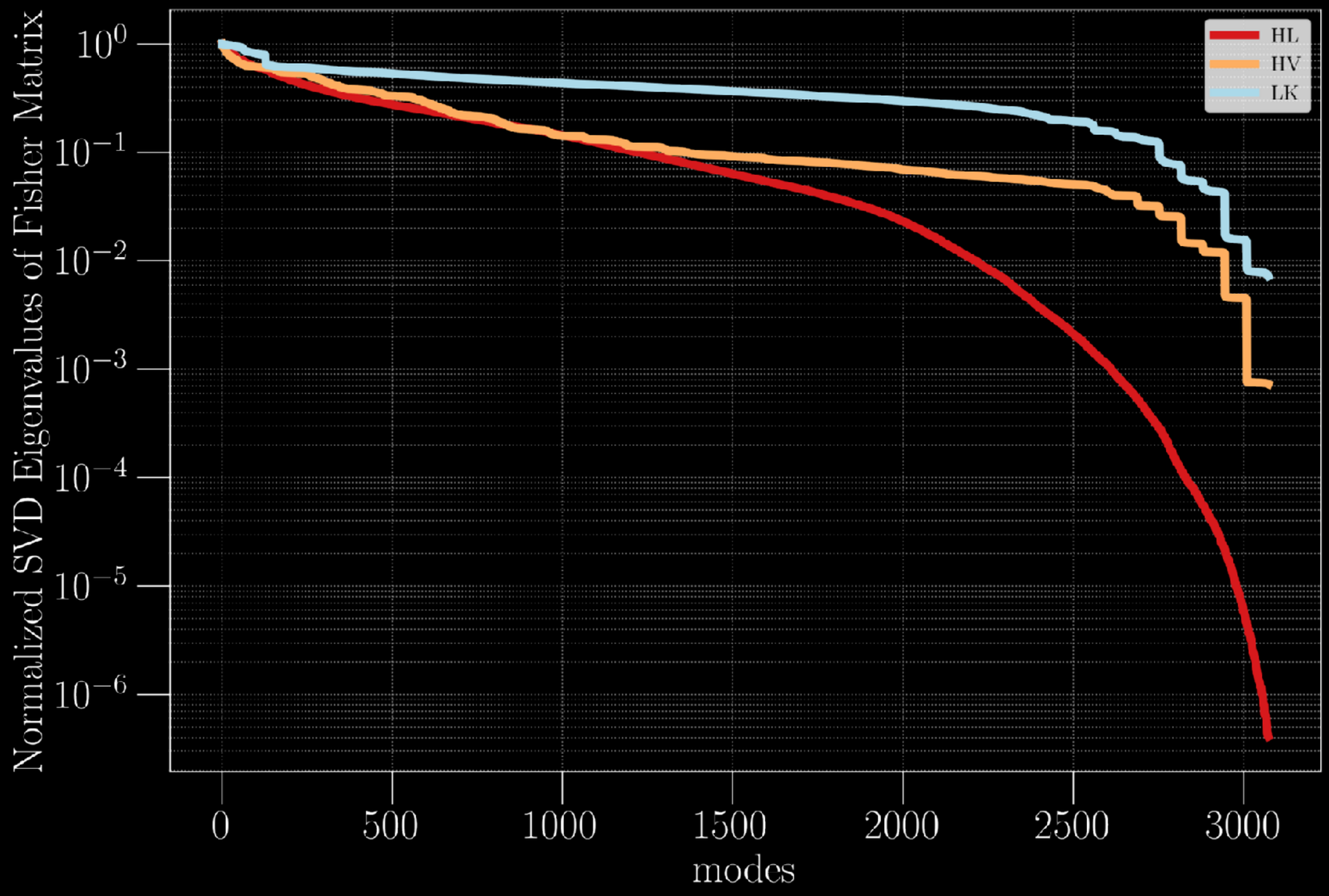

ADDING MORE DETECTORS

Increasing the number of baselines considered in the analysis will act as a natural regulariser of the Fisher Matrix.

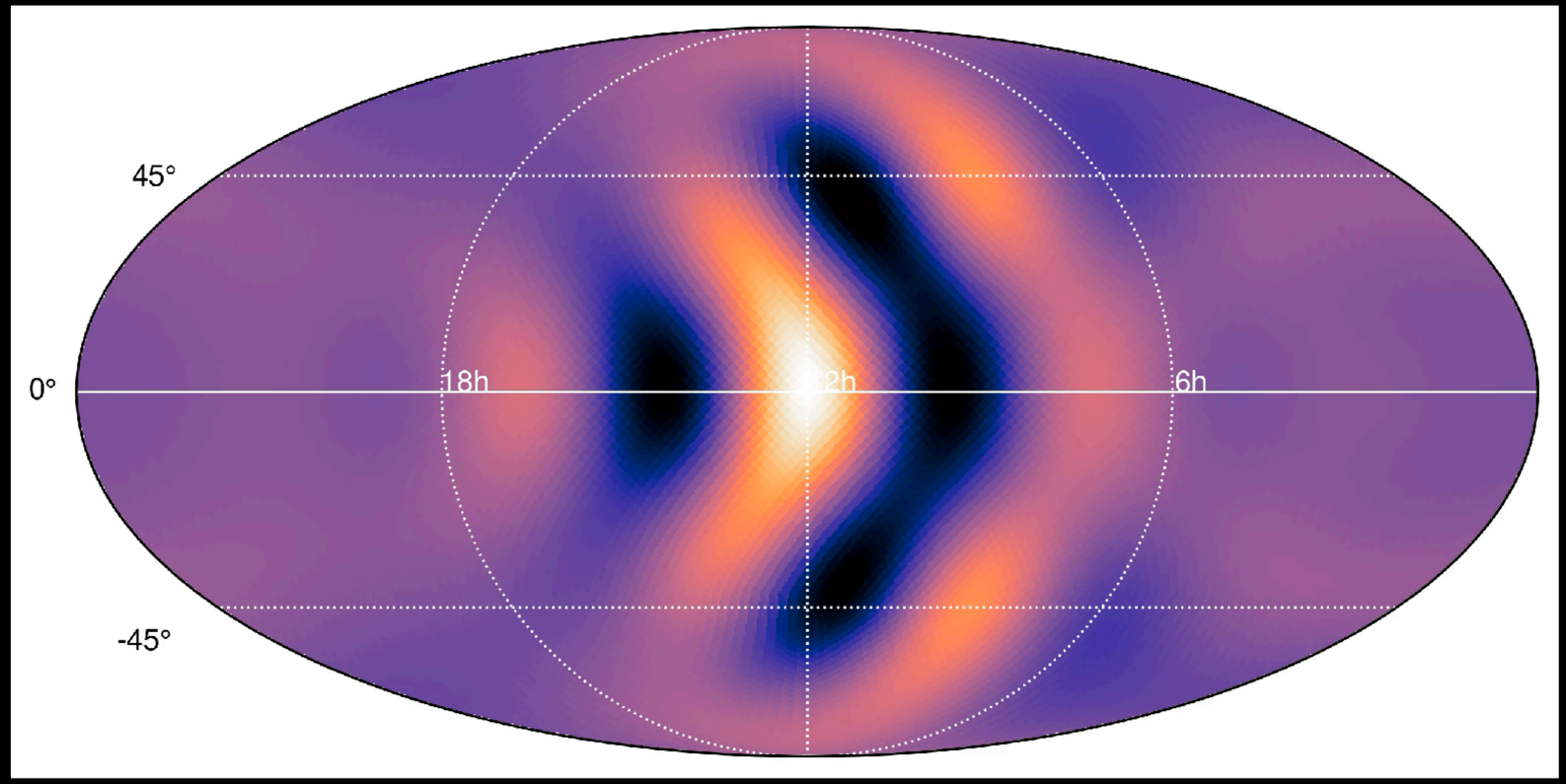

ADDING MORE DETECTORS

Increasing the number of baselines considered in the analysis will act as a natural regulariser of the Fisher Matrix.

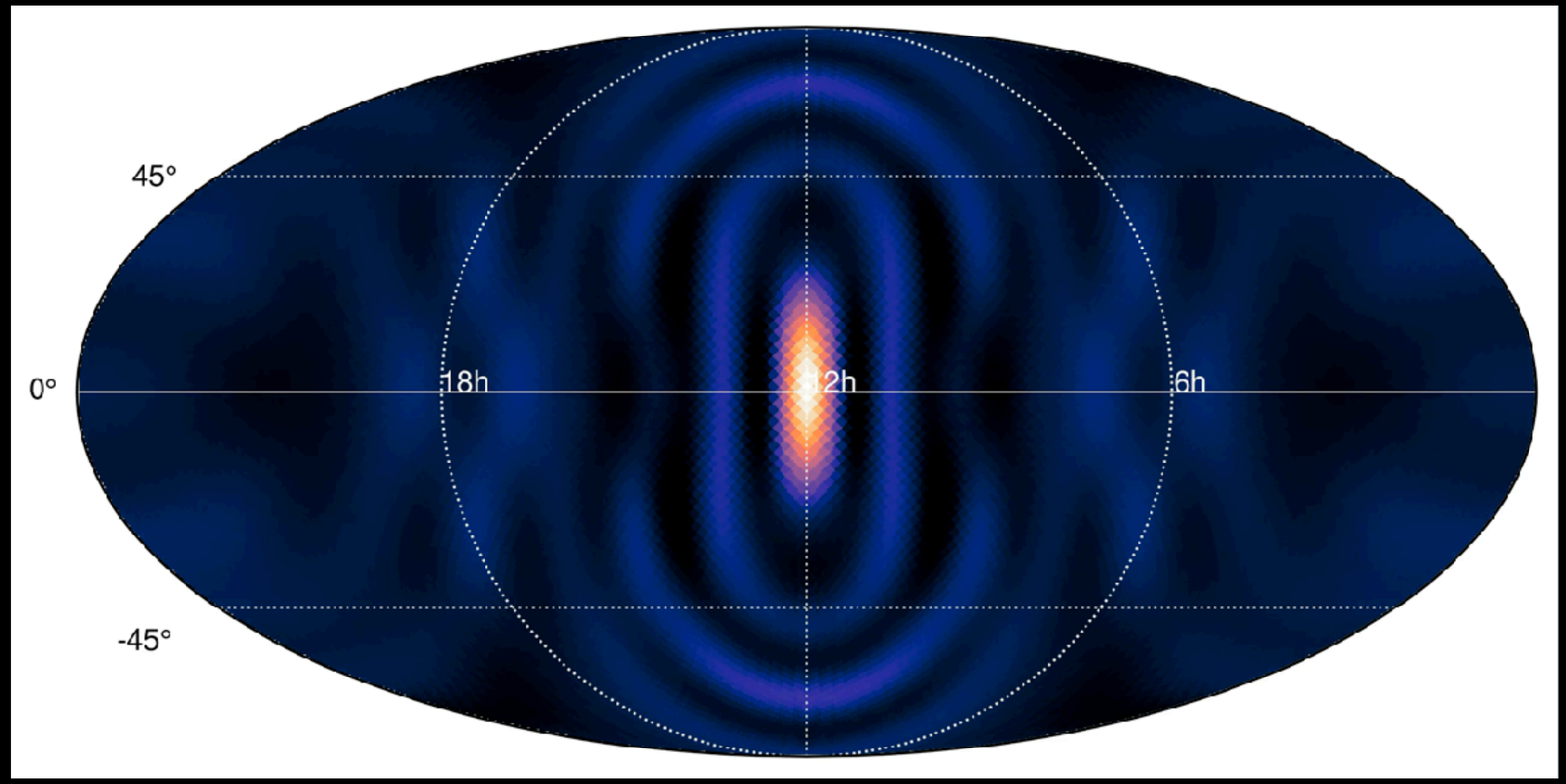

REGULARIZATION SCHEMES

$$\mathbf{\Gamma}_R = \mathbf{V}\,\mathbf{S}_R\,\mathbf{U}^\dagger$$

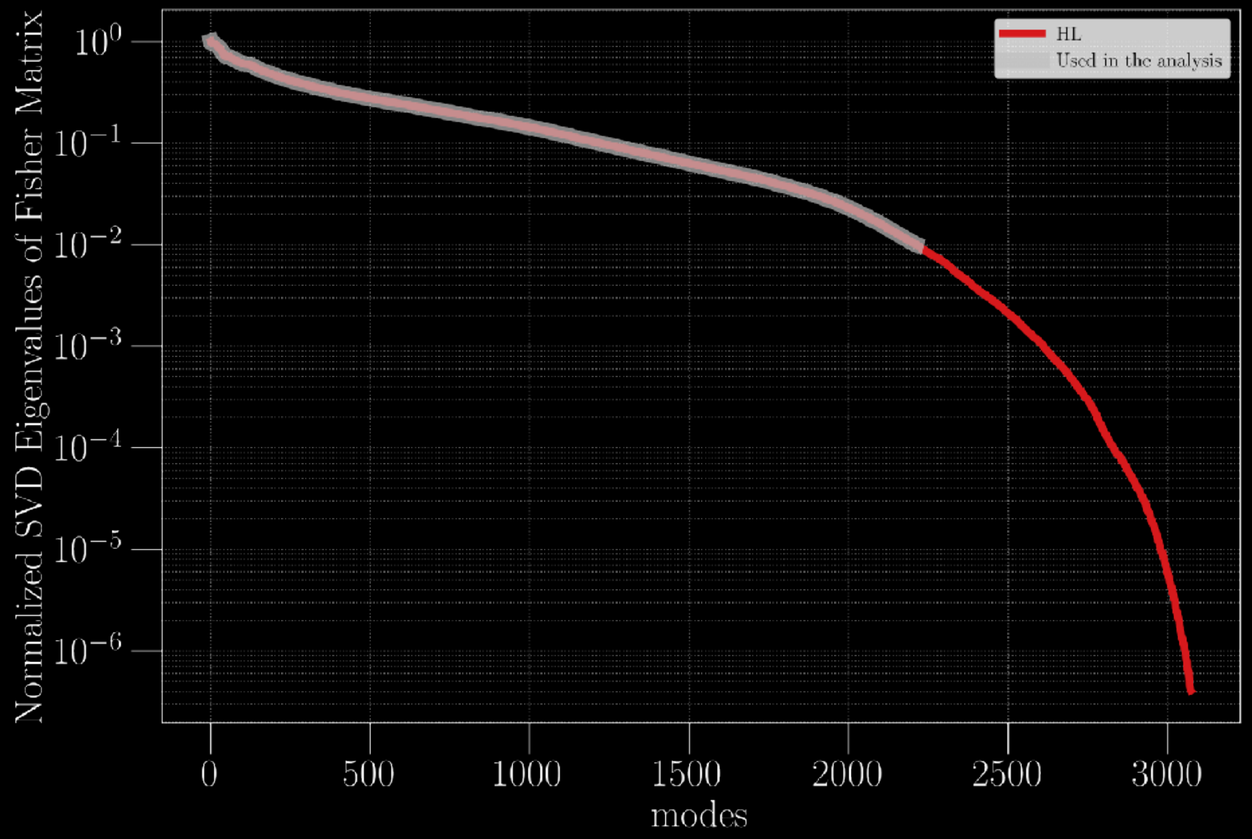

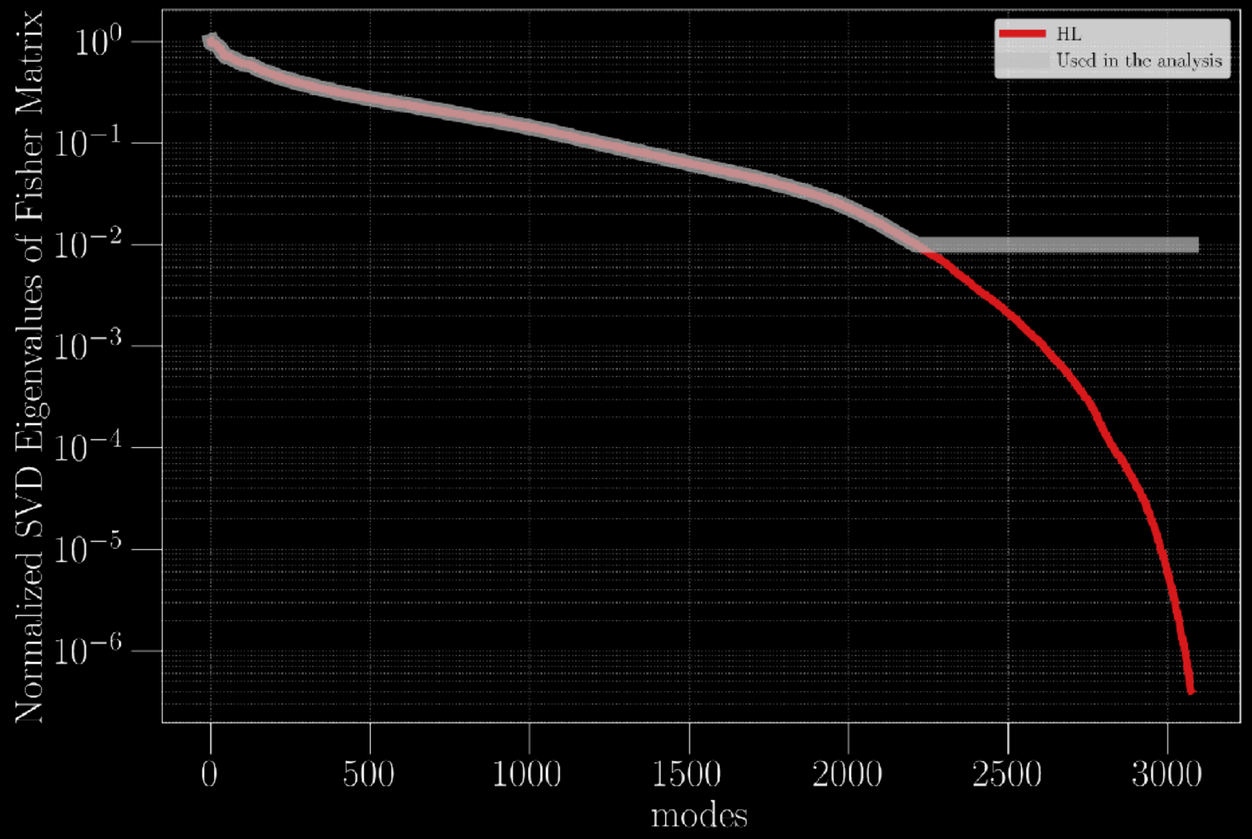

Regularization introduces bias. So one has to consider a proper trade-off between the bias—variance—condition number.

This makes the deconvolution problem trickier.

For more details:

E. Thrane et al., PRD 80, 122002 (2009)
S. Panda et al., PRD 100, 043541 (2019)
D. Agarwal et al., PRD 104, 123018 (2021)

ONCE WE REACH THE DETECTION THRESHOLD……!

Let us consider our usual analysis, where $\mathscr{P}(f, \hat{\Omega}) = H(f)\,\mathscr{P}(\hat{\Omega})$

spectral shape of the background

In usual single-component analysis, we assume a fiducial model for the spectral shape and perform the optimal filtering.

usually consider a power-law format, $H(f) = \left(\frac{f}{f_{\rm ref}}\right)^{\alpha-3}$

If we filter the data for each GWB component separately (like above): we overestimate the amplitude of each GWB component and underestimate the error bars.

We must go beyond the single-component analysis to better extract the amplitudes of individual GWB components*.

* Ungarelli+ PRD 64,121501 (2001), V. Mandic+ PRL 109, 171102 (2012), K. Martinovic+PRD 103,043023 (2021), G. Boileau+PRD 103, 103529 (2021)

MULTI-COMPONENT, JOINT-ANALYSIS

Parida+JCAP 04, 024 (2016)

Suresh+PRD 104, 102003 (2021)

Fisher information matrix-based method to jointly estimate the GWB components.

These methods are explored in detail for isotropic searches. FDL+ (in-preparation)

Let's consider a multi-component anisotropic SGWB

$$\mathscr{P}(f,\hat{\Omega}) = \sum_{\alpha} H_{\alpha}(f)\,\mathscr{P}^{\alpha}(\hat{\Omega})$$

Spectral-shape of different backgrounds

From the maximum-likelihood statistics: $\hat{\mathscr{P}}^{\alpha}_{u} = \mathbf{\Gamma}^{-1}\cdot\mathbf{X}$

Dirty map $$\mathbf{X} \equiv X^{\alpha}_{u} = \sum_{ft} \gamma^{*}_{ft,u}\,\frac{H_{\alpha}(f)}{P_1(t;f)P_2(t;f)}\,\mathscr{C}(t;f)$$

Fisher information matrix $$\mathbf{\Gamma} \equiv \Gamma^{\alpha\beta}_{uu'} = \sum_{ft} \frac{H_{\alpha}(f)H_{\beta}(f)}{P_1(t;f)\,P_2(t;f)}\,\gamma^{*}_{ft,u}\,\gamma_{ft,u'}$$

(noise-weighted inner product of spectral shapes)

MULTI-COMPONENT, JOINT-ANALYSIS

For a three-spectral index case,
we can write the ML solution as

$$\begin{bmatrix} X_u^{\alpha 1} \\ X_u^{\alpha 2} \\ X_u^{\alpha 3} \end{bmatrix} = \begin{bmatrix} \Gamma_{uu'}^{\alpha 1 \alpha 1} & \Gamma_{uu'}^{\alpha 1 \alpha 2} & \Gamma_{uu'}^{\alpha 1 \alpha 3} \\ \Gamma_{uu'}^{\alpha 2 \alpha 1} & \Gamma_{uu'}^{\alpha 2 \alpha 2} & \Gamma_{uu'}^{\alpha 2 \alpha 3} \\ \Gamma_{uu'}^{\alpha 3 \alpha 1} & \Gamma_{uu'}^{\alpha 3 \alpha 2} & \Gamma_{uu'}^{\alpha 3 \alpha 3} \end{bmatrix} \begin{bmatrix} \hat{\mathscr{P}}_{u'}^{\alpha 1} \\ \hat{\mathscr{P}}_{u'}^{\alpha 2} \\ \hat{\mathscr{P}}_{u'}^{\alpha 3} \end{bmatrix}$$

Coupling Matrix

$$\hat{\mathscr{P}}_u^{\alpha} = \sum_{u'\beta} \left[C^{-1}\right]_{uu'}^{\alpha\beta} X_{u'}^{\beta}$$

MULTI-COMPONENT, JOINT-ANALYSIS

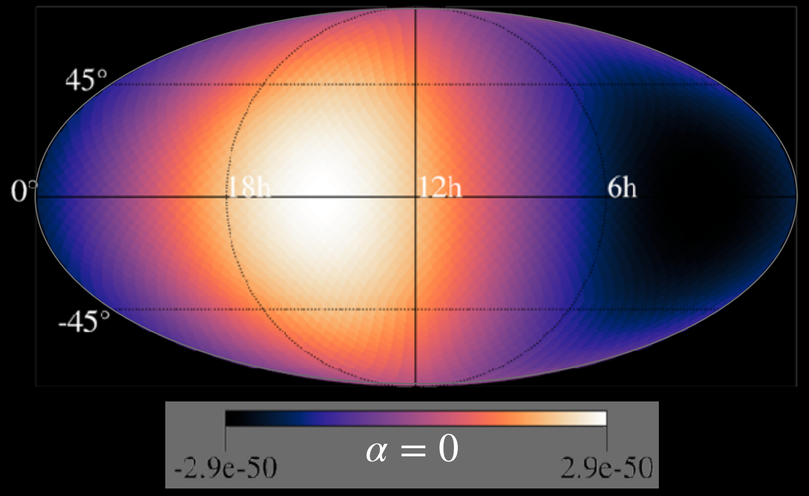

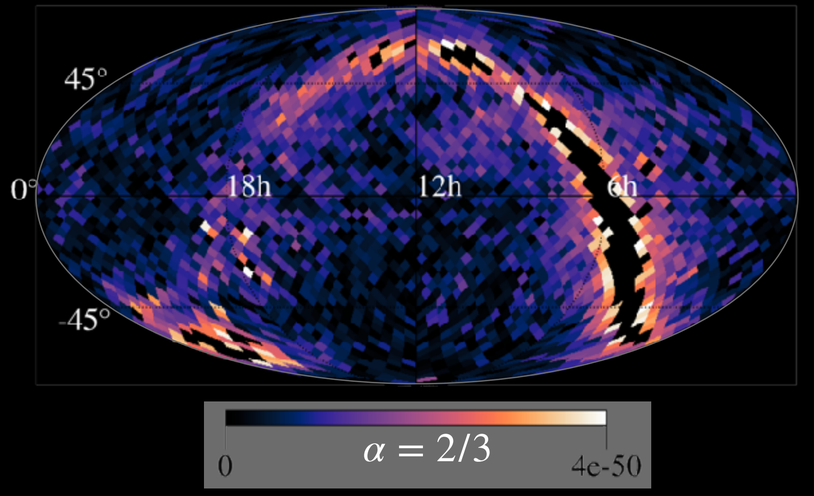

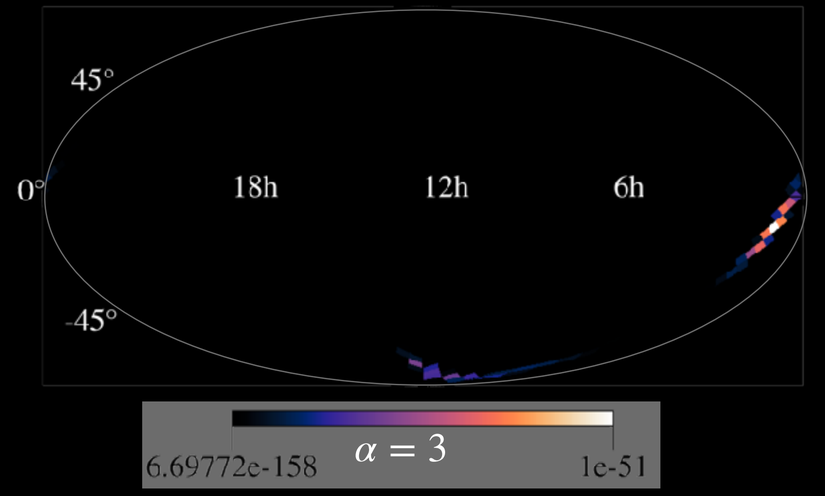

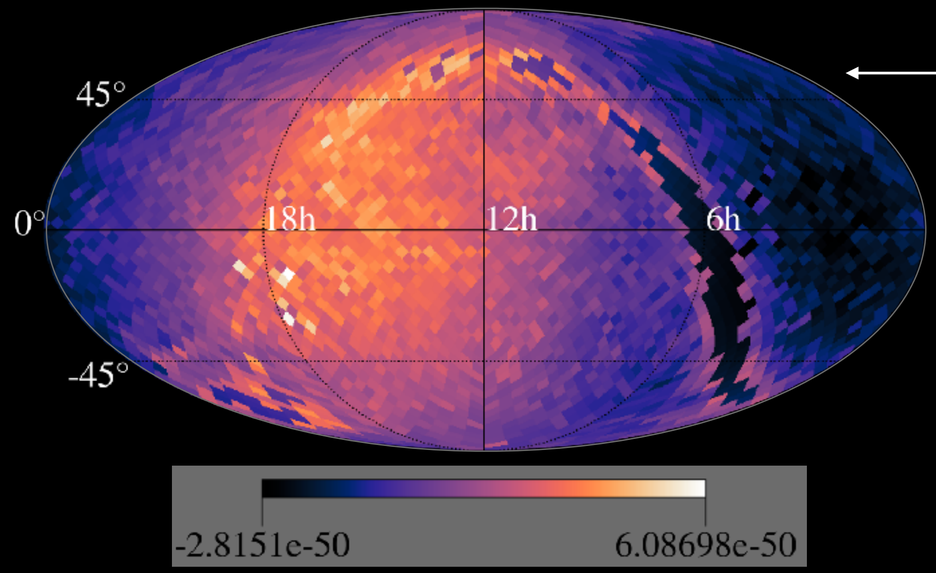

Combined Source

Coupling Matrix

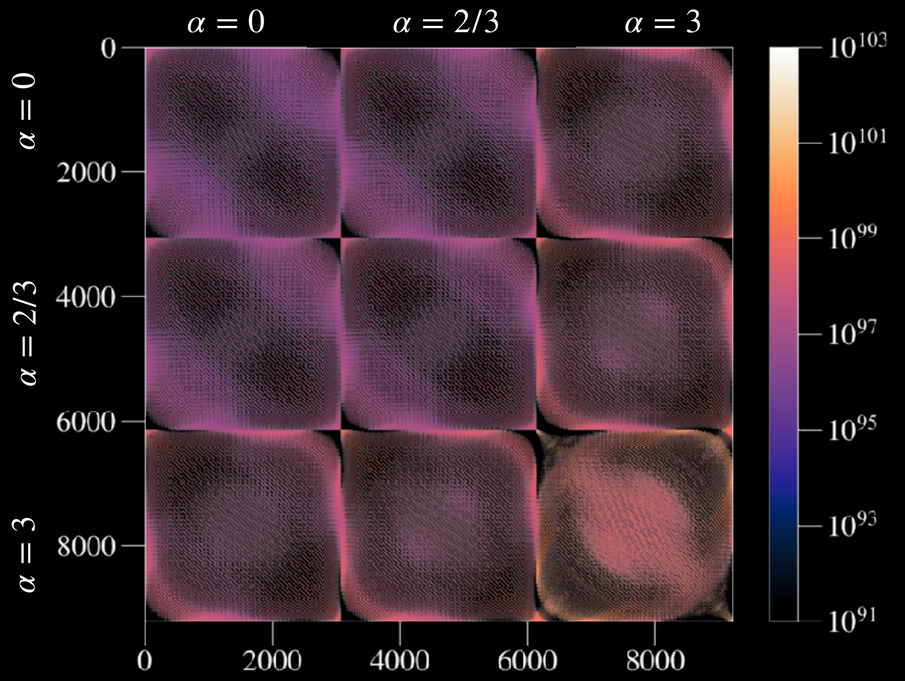

MULTI-COMPONENT, JOINT-ANALYSIS

Suresh+PRD 104, 102003 (2021)

Single-Index analysis

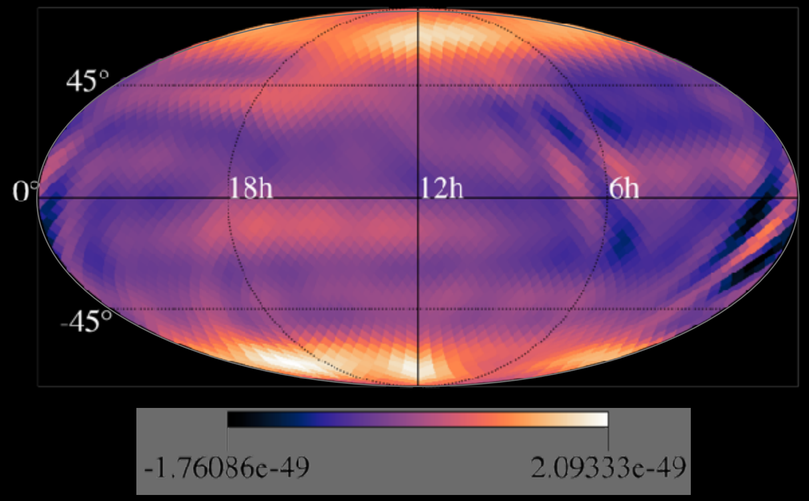

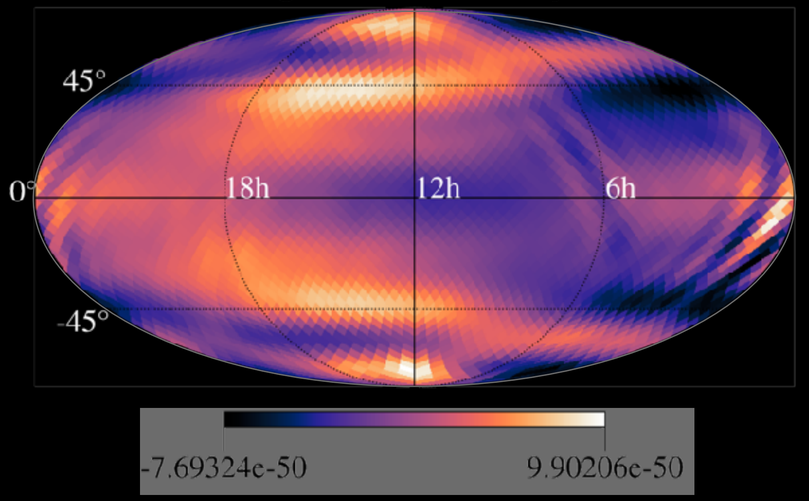

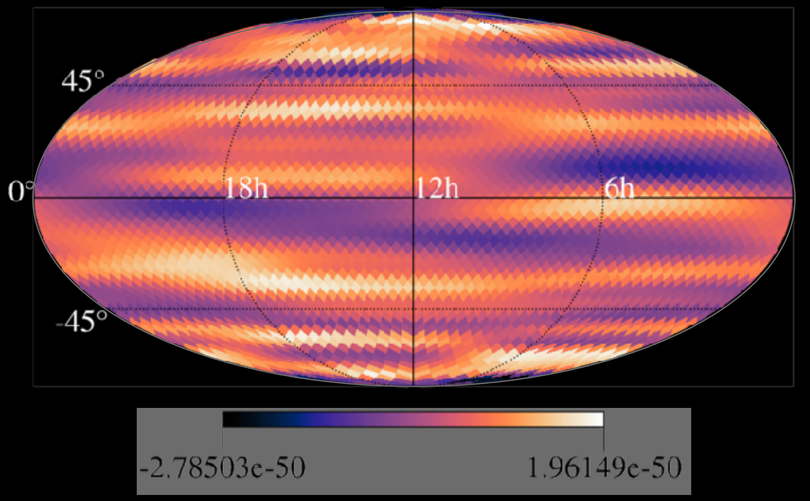

Multi-Index analysis

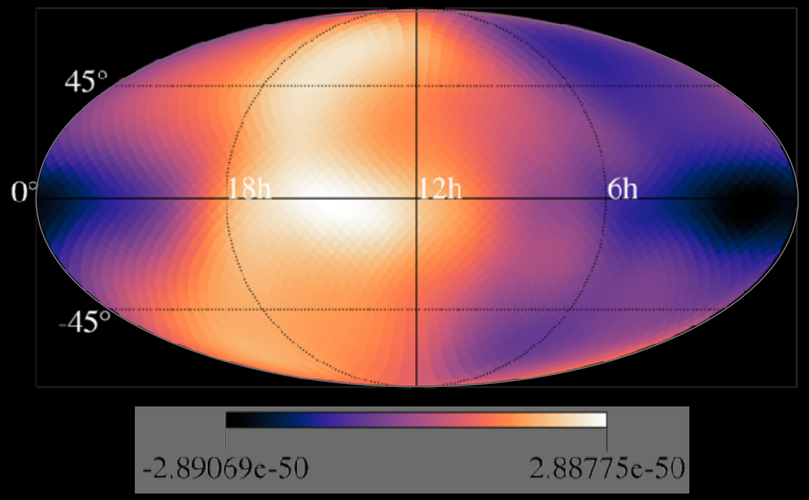

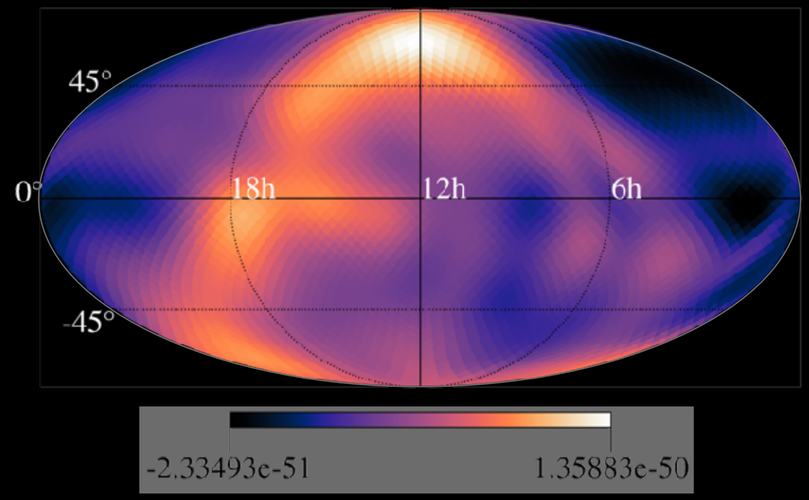

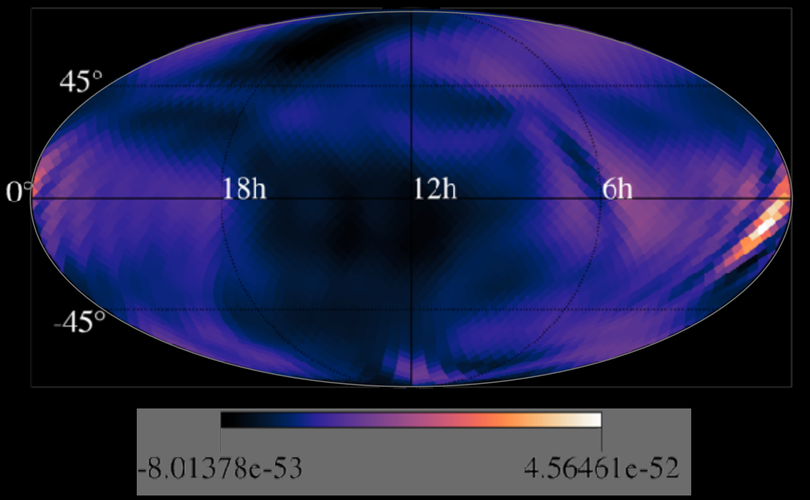

MULTI-COMPONENT, JOINT-ANALYSIS

Suresh+PRD 104, 102003 (2021)

Upper Limit: O1+O2+O3

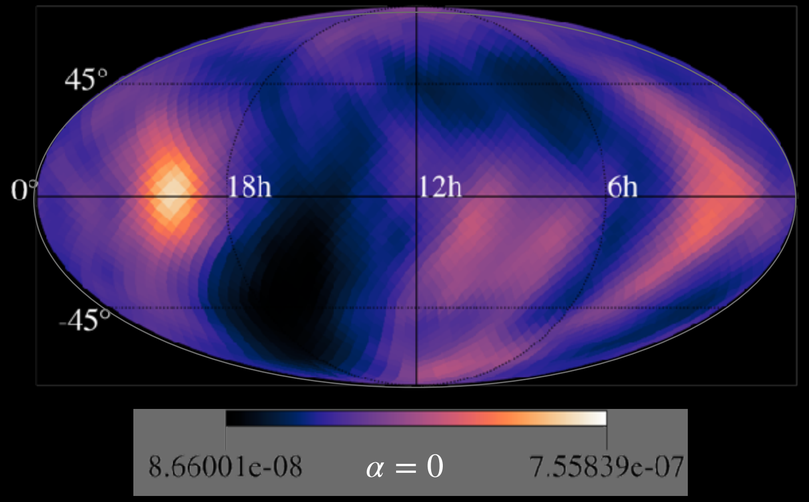

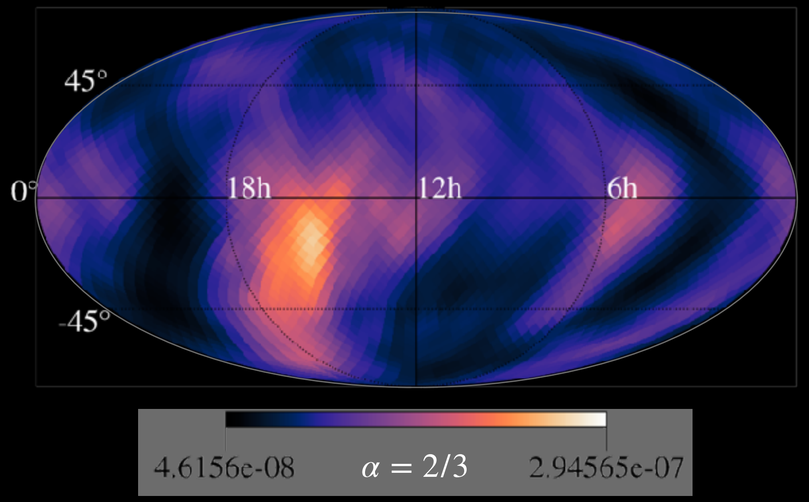

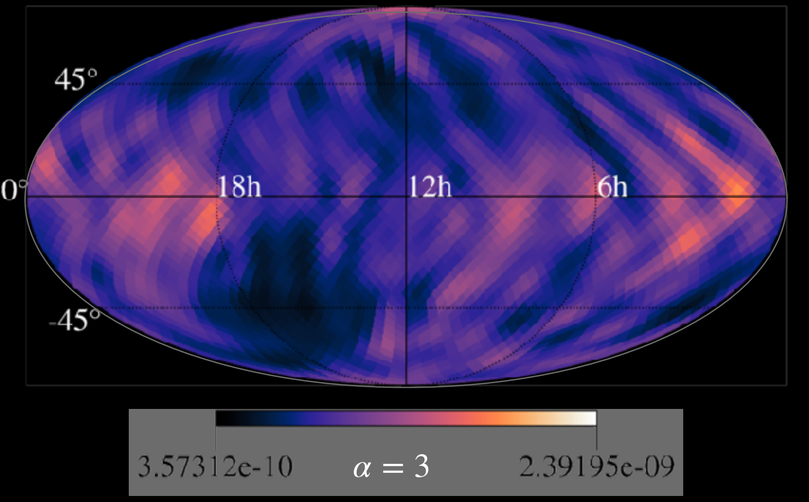

95% Upper Limit $\times 10^{-8}$					
α	Single Index	Joint Index			
		two-α			three-α
		0 , 2/3	0 , 3	2/3 , 3	
0	2.89-11.8	7.05-57.84	2.71-13.07		8.66-75.58
2/3	1.38-6.35	3.85-19.66		1.52-7.45	4.62-29.45
3	0.024-0.157		0.023-0.165	0.025-0.18	0.036-0.24

- Joint analysis accurately separates and estimates backgrounds with different spectral shapes and different sky distributions with no major bias.
- The upper limits set by the joint analysis are safer, though less strict than the individual analysis.

WE ARE NOW AT:

adapted from LIGO S4 paper: APJ 659:918, 2007

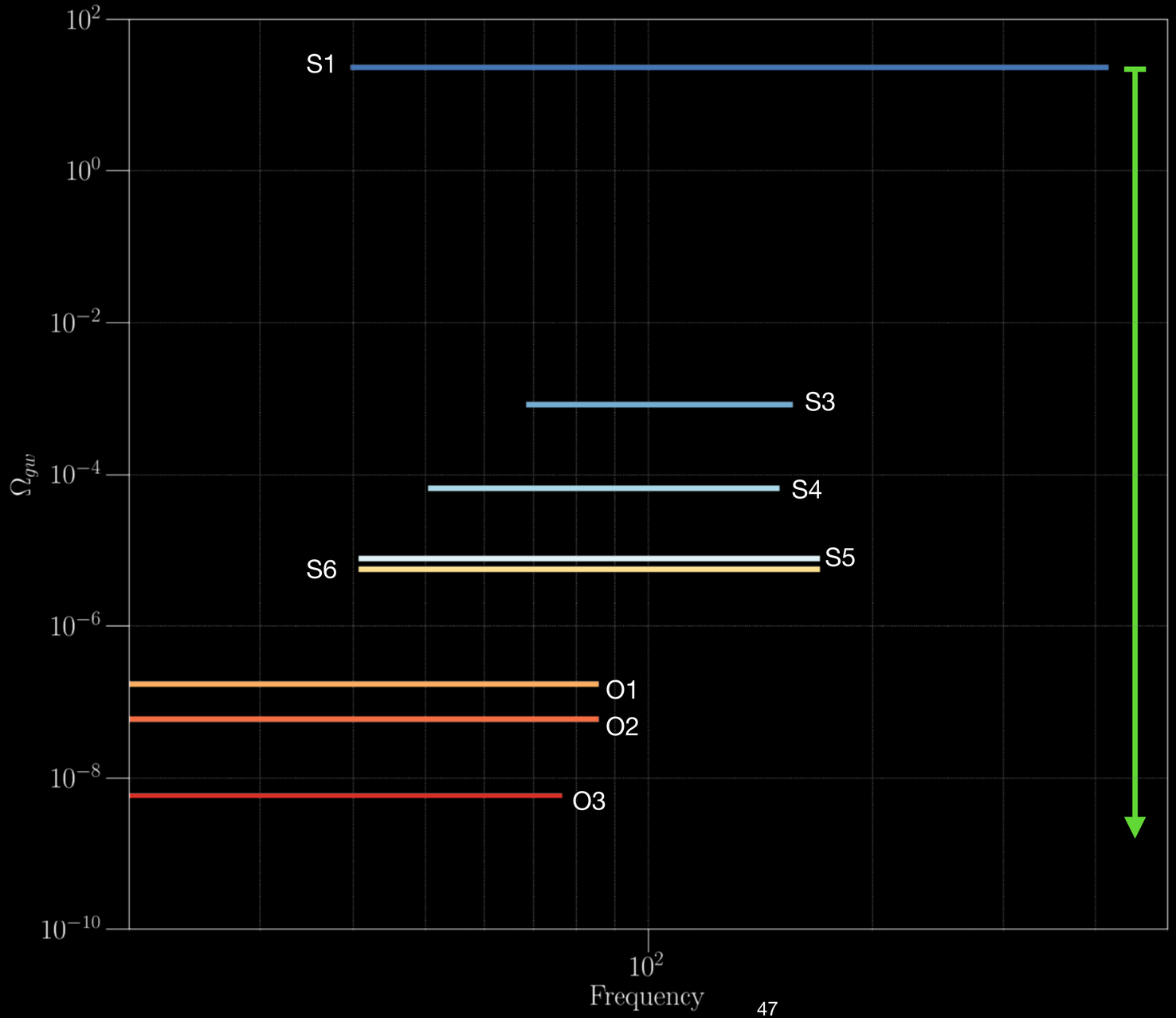

Long road ahead…..

- New searches and techniques are opening up efficient ways to probe the dark universe.
- Plenty more work to do!
    - More detectors, More signals, More systems, and Dealing with real data…..

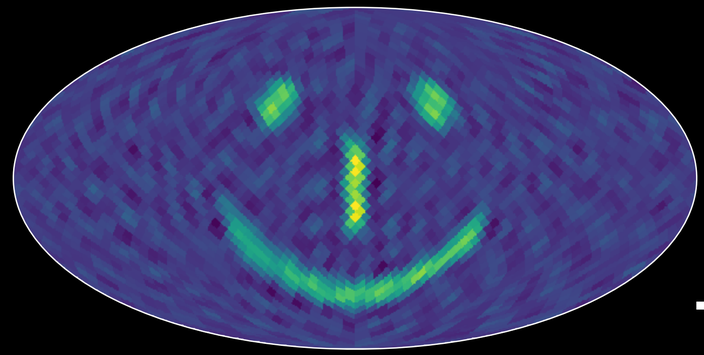

Thank you!

★ pygwb –> pip install pygwb
PyStoch –> pip install pystoch (beta version)

BACKUP

GRAVITATIONAL WAVE ORCHESTRA

SEPTEMBER 08-09, 2022

UNIVERSITÉ CATHOLIQUE DE LOUVAIN, BELGIUM

GWO

Current and Future Stochastic Gravitational-Wave Background Probes in Multiple Frequency Bands

- Review on stochastic gravitational-wave background searches
- Theoretical developments in stochastic background modelling
- Most updated results from:
  LIGO-Virgo-KAGRA collaboration and Pulsar Timing Arrays
- Future probes and strategies using:
  Einstein Telescope, Cosmic Explorer, and LISA

GRAVITATIONAL WAVE ORCHESTRA 2024

SEPTEMBER 2024 (?)

Venue: Three Potential Host Institutes

1. LAPP, Annecy
2. UMN, Minnesota
3. UCLouvain, Louvain-la-Neuve

Plans:

1. SGWB probes in different frequency bands: Overview Talks
2. Contributed talks from Early Carrier Scientists
3. Hands-on session –> Most of the SGWB search tools are publicly available. We plan to have hands-on sessions every afternoon.

Mark your calendar and Stay tuned!

FOLDING

- The estimator (“dirty map”)

$$X_\alpha = \sum_{Ift} K^{I*}_{\alpha,ft} \left[\sigma^{-2}_{Ift}\, C^I_{ft} \;-\; \frac{1}{2}\varepsilon^I_{t-1} \left\{ \sigma^{-2}_{Ift} + \sigma^{-2}_{If(t-1)} \right\} C^I_{f(t-1)} \right.$$
$$\left. -\; \frac{1}{2}\varepsilon^I_{t+1} \left\{ \sigma^{-2}_{Ift} + \sigma^{-2}_{If(t+1)} \right\} C^I_{f(t+1)} \right]$$

$$= \sum_{Ift_{sid}} K^{I*}_{\alpha,ft_{sid}} \sum_{i_{day}} \left[\sigma^{-2}_{If(i_{day}+t_{sid})}\, C^I_{f(i_{day}+t_{sid})} \right.$$

$$- \; \frac{1}{2}\varepsilon^I_{i_{day}+t_{sid}-1} \left\{ \sigma^{-2}_{If(i_{day}+t_{sid})} + \sigma^{-2}_{If(i_{day}+t_{sid}-1)} \right\} C^I_{f(i_{day}+t_{sid}-1)}$$

$$\left. - \; \frac{1}{2}\varepsilon^I_{i_{day}+t_{sid}+1} \left\{ \sigma^{-2}_{If(i_{day}+t_{sid})} + \sigma^{-2}_{If(i_{day}+t_{sid}+1)} \right\} C^I_{f(t_{sid}+t_{sid}+1)} \right]$$

- The Fisher information matrix (three data streams)

$$\Gamma_{\alpha\alpha'} = \sum_{Ift} K^{I*}_{\alpha,ft} \left[\sigma^{-2}_{Ift}\, K^I_{ft,\alpha'} \;-\; \frac{1}{2}\varepsilon^I_{t-1} \left\{ \sigma^{-2}_{Ift} + \sigma^{-2}_{If(t-1)} \right\} K^I_{f(t-1),\alpha'} \right.$$
$$\left. -\; \frac{1}{2}\varepsilon^I_{t+1} \left\{ \sigma^{-2}_{Ift} + \sigma^{-2}_{If(t+1)} \right\} K^I_{f(t+1),\alpha'} \right]$$

$$= \sum_{Ift_{sid}} K^{I*}_{\alpha,ft_{sid}}\, K^I_{ft_{sid},\alpha'} \sum_{i_{day}} \sigma^{-2}_{If(i_{day}+t_{sid})}$$

$$- \sum_{Ift_{sid}} K^{I*}_{\alpha,ft_{sid}}\, K^I_{f(t_{sid}-1),\alpha'} \sum_{i_{day}} \frac{1}{2}\varepsilon^I_{i_{day}+t_{sid}-1} \left\{ \sigma^{-2}_{If(i_{day}+t_{sid})} + \sigma^{-2}_{If(i_{day}+t_{sid}-1)} \right\}$$

$$- \sum_{Ift_{sid}} K^{I*}_{\alpha,ft_{sid}}\, K^I_{f(t_{sid}+1),\alpha'} \sum_{i_{day}} \frac{1}{2}\varepsilon^I_{i_{day}+t_{sid}+1} \left\{ \sigma^{-2}_{If(i_{day}+t_{sid})} + \sigma^{-2}_{If(i_{day}+t_{sid}+1)} \right\}$$

O3 CSD

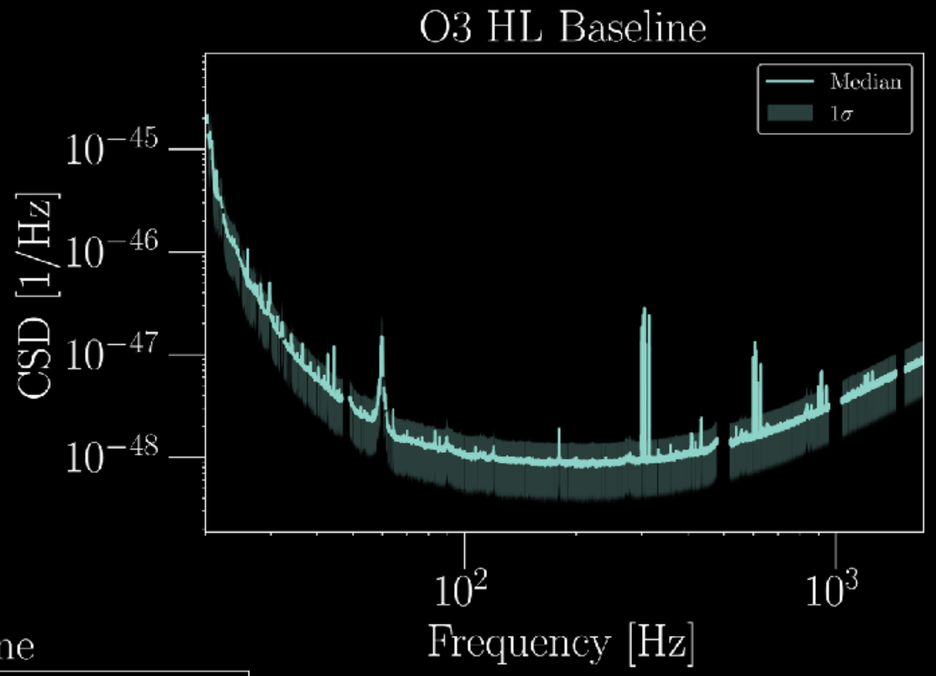
O3 HL Baseline
Median
1σ
CSD [1/Hz]
10^{-45}
10^{-46}
10^{-47}
10^{-48}
10^{2}
10^{3}
Frequency [Hz]

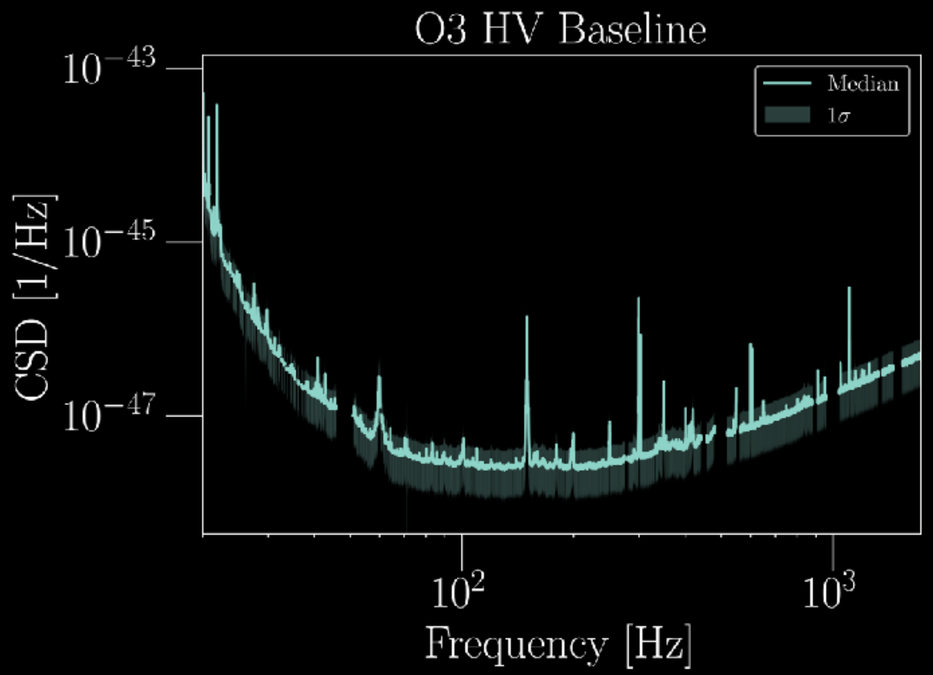
O3 HV Baseline
Median
1σ
CSD [1/Hz]
10^{-43}
10^{-45}
10^{-47}
10^{2}
10^{3}
Frequency [Hz]

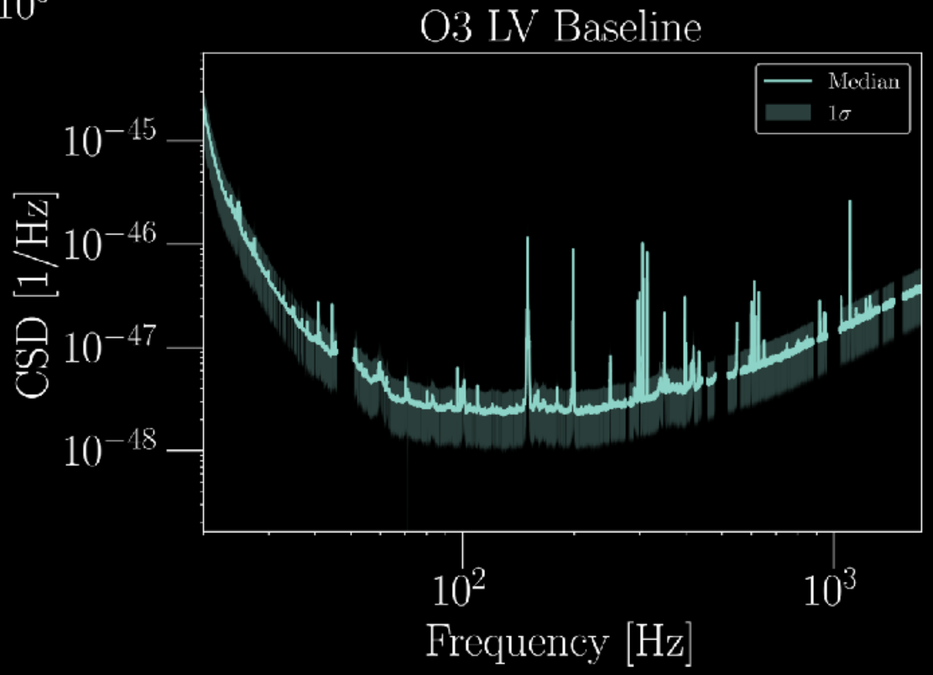
O3 LV Baseline
Median
1σ
CSD [1/Hz]
10^{-45}
10^{-46}
10^{-47}
10^{-48}
10^{2}
10^{3}
Frequency [Hz]

ANALYSIS OVERVIEW

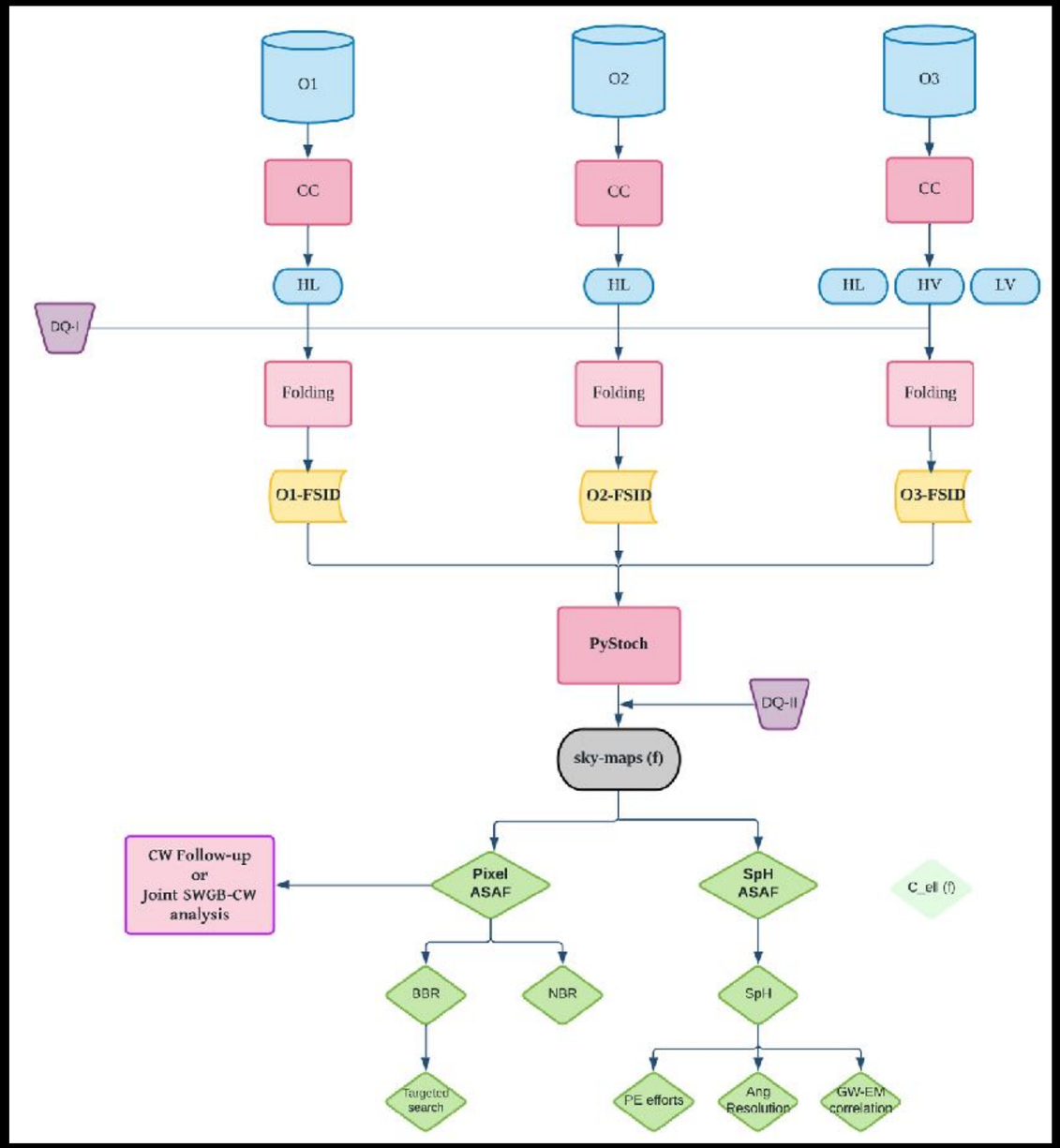

O3 ANISOTROPIC RESULT

PRD 104, 022005 (2021)

- Broadband: point sources with different power-law spectra.
- Narrowband: point sources having narrow GW frequency band (SN 1987A, ScoX-1, GC)
- Spherical harmonics search: Extended or diffuse sources - measure angular power spectra

All-sky BBR Results

			Max SNR (% p-value)				Upper limit ranges (10^{-8})	
α	Ω_{GW}	$H(f)$	**HL(O3)**	**HV(O3)**	**LV(O3)**	O1 + O2 + O3 **(HLV)**	O1 + O2 + O3 **(HLV)**	O1 + O2 **(HL)**
0	Constant	$\propto f^{-3}$	2.3 (66)	3.4 (24)	3.1 (51)	2.6 (23)	1.7–7.6	4.4–21
$2/3$	$\propto f^{2/3}$	$\propto f^{-7/3}$	2.5 (59)	3.7 (14)	3.1 (62)	2.7 (24)	0.85–4.1	2.3–12
3	$\propto f^{3}$	Constant	3.7 (32)	3.6 (47)	4.1 (12)	3.6 (20)	0.013–0.11	0.046–0.32

O3 ANISOTROPIC RESULT

PRD 104, 022005 (2021)

- Broadband: point sources with different power-law spectra.
- Narrowband: point sources having narrow GW frequency band (SN 1987A, ScoX-1, GC)
- Spherical harmonics search: Extended or diffuse sources - measure angular power spectra

Narrow band Radiometer Results

Direction	Max SNR	p-value (%)	Frequency (Hz) (± 0.016 Hz)	Best upper limit (10^{-25})	Frequency band (Hz)
Scorpius X-1	4.1	65.7	630.31	2.1	189.31–190.31
SN 1987A	4.9	1.8	414.0	1.7	185.13–186.13
Galactic Center	4.1	62.3	927.25	2.1	202.56–203.56

O3 ANISOTROPIC RESULT

PRD 104, 022005 (2021)

- Broadband: point sources with different power-law spectra.
- Narrowband: point sources having narrow GW frequency band (SN 1987A, ScoX-1, GC)
- Spherical harmonics search: Extended or diffuse sources - measure angular power spectra

SHD Results

			Max SNR (% p-value)				Upper limit range (10^{-9})	
α	$\Omega_{\rm GW}$	$H(f)$	**HL(O3)**	**HV(O3)**	**LV(O3)**	O1 + O2 + O3 **(HLV)**	O1 + O2 + O3 **(HLV)**	O1 + O2 **(HL)**
0	Constant	$\propto f^{-3}$	1.6 (78)	2.1 (40)	1.5 (83)	2.2 (43)	3.2–9.3	7.8–29
$2/3$	$\propto f^{2/3}$	$\propto f^{-7/3}$	3.0 (13)	3.9 (0.98)	1.9 (82)	2.9 (18)	2.4–9.3	6.4–25
3	$\propto f^{3}$	Constant	3.9 (12)	4.0 (10)	3.9 (11)	3.2 (60)	0.57–3.4	1.9–11

HISTOGRAM OF SNR –> SPH ANALYSIS

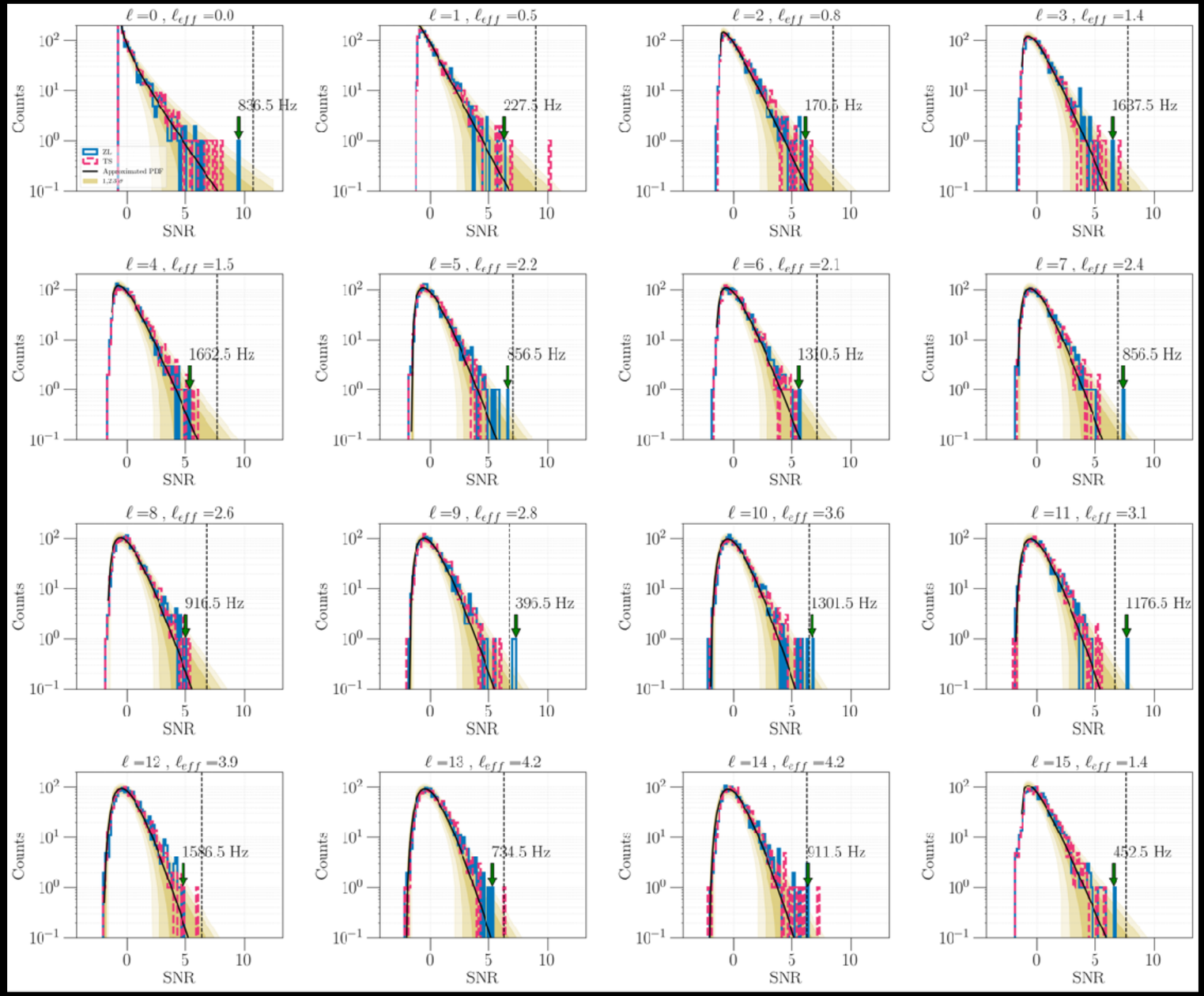

Here, for each harmonic mode, the frequency samples are treated as independent samples for the statistic. The solid black line represents the approximate PDF with effective DOF $k_{\text{eff}} = 2\ell_{\text{eff}} + 1$ best fitted to the samples obtained by the time-shifted run. The zero-lag and time-shifted data is broadly consistent with the approximated distribution of SNRs within three-sigma (yellow colour) Poisson error bars for lower harmonic modes but deviate at higher modes. The frequencies for maximum SNR in the zero-lag run are indicated in the histogram. The black dashed line depicts the SNR threshold for the global p-value 0.05 given approximated PDF

We note that the null distribution of SNR, the estimators of the angular power spectra, is no longer Gaussian.

COMPONENT SEPARATION

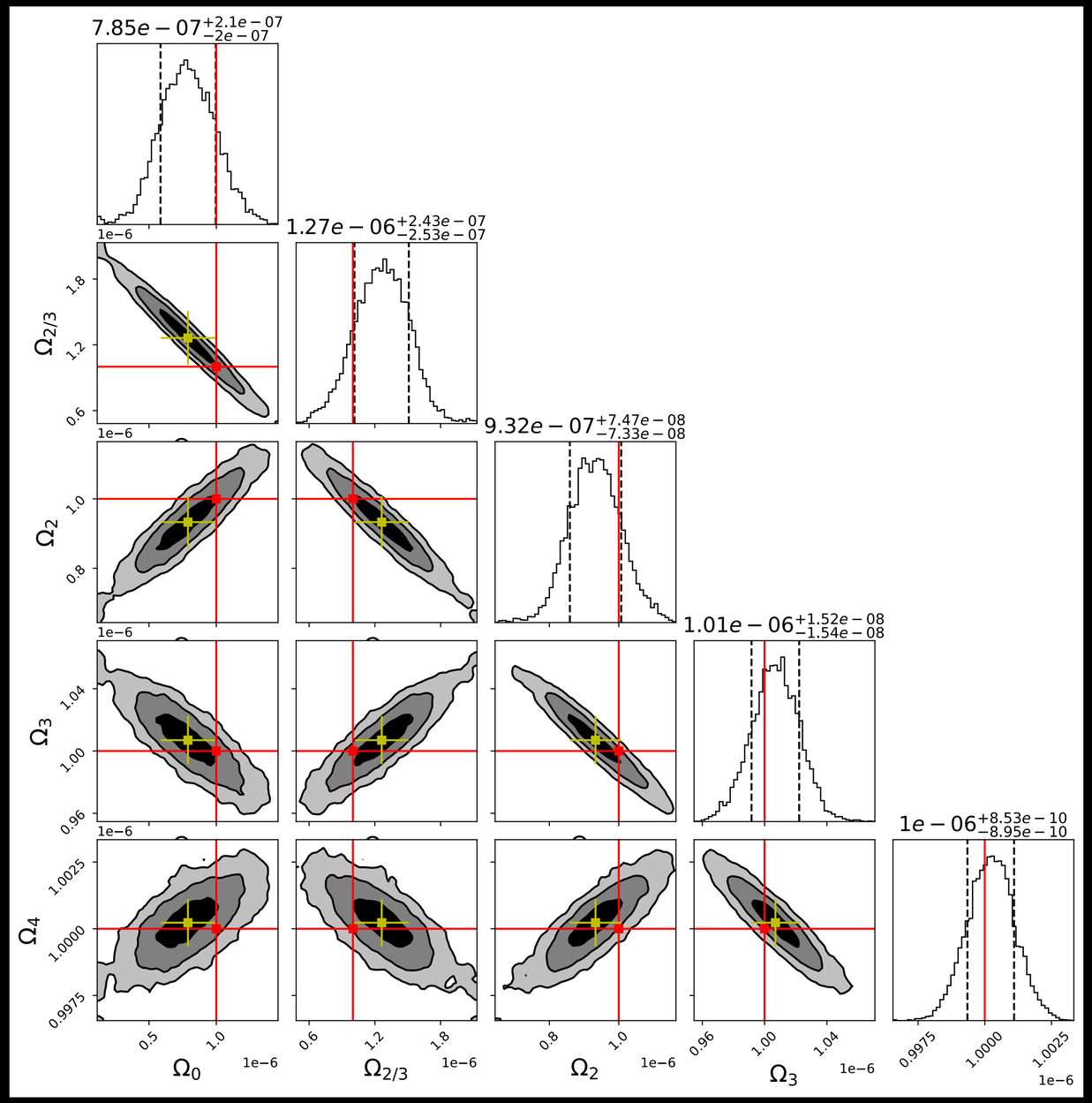

Astrophysical components and Jointly analysing the total background

Injection Studies

$\alpha = 0$ | $\alpha = 2/3$ | $\alpha = 3$

Estimated Amplitude

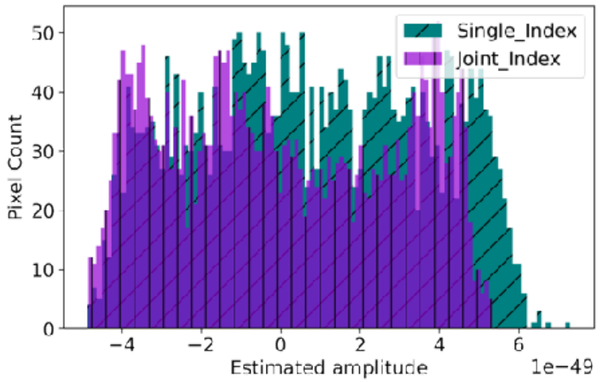

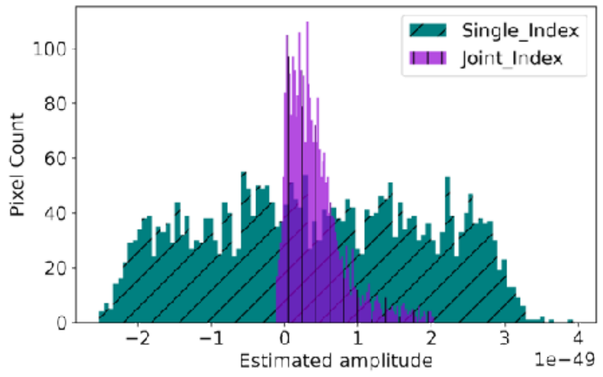

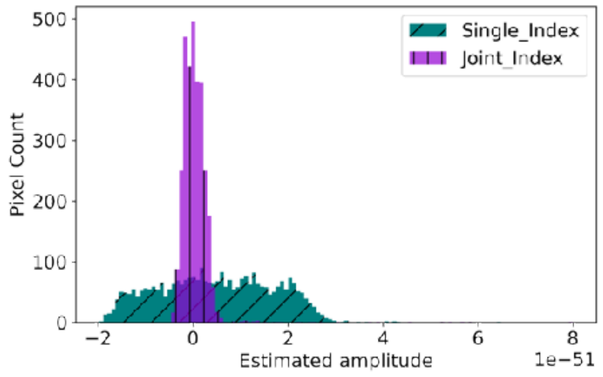

Variance

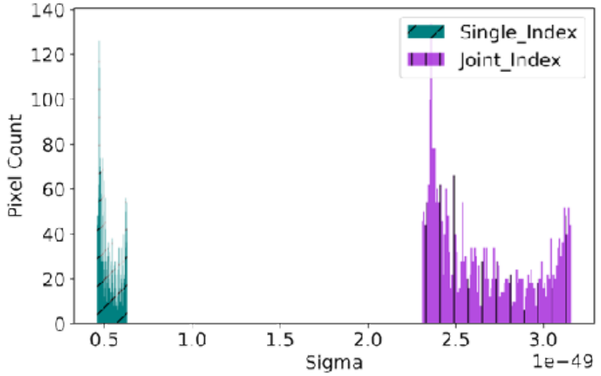

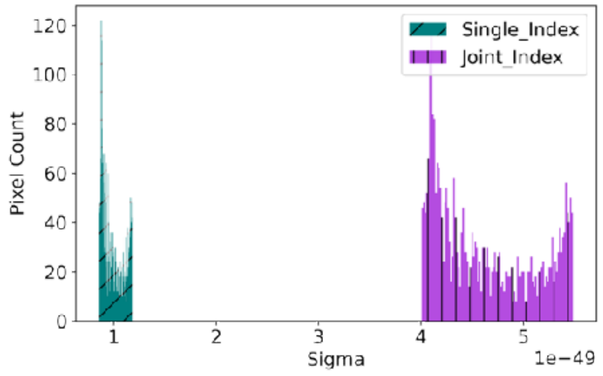

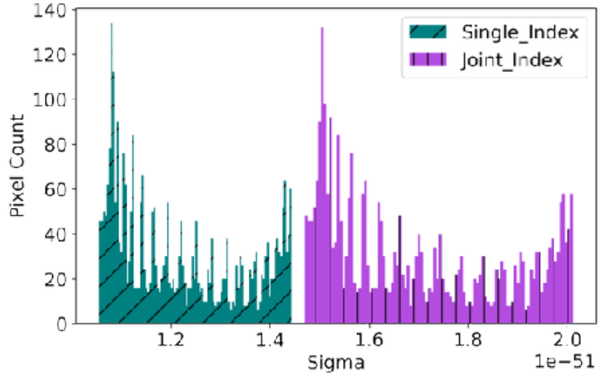

95% confident UL - Injection

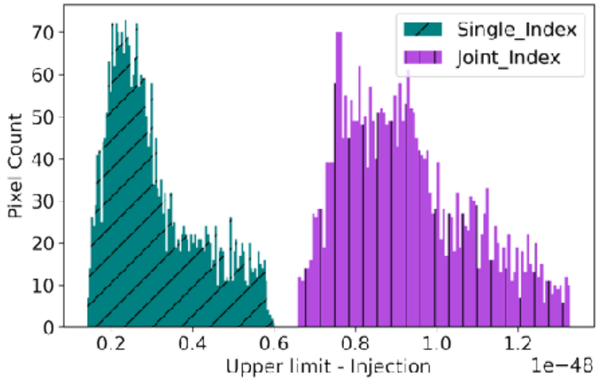

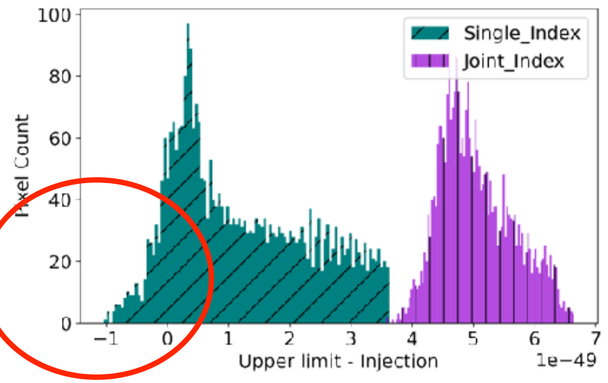

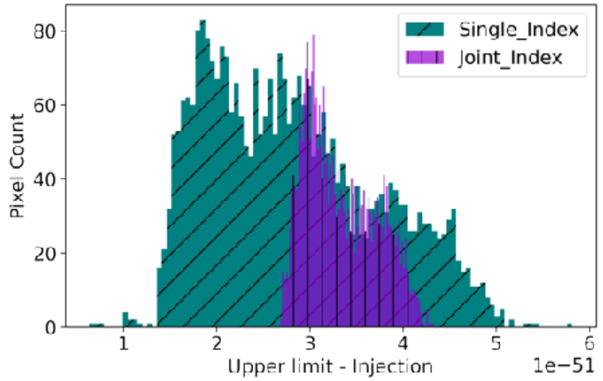

11% of the points in the histogram fall under the negative region

Upper limit from injection study

- Produced UL sky maps corresponding to the injection (injection strength is set to be close to the detectable limit).
- Histogram shows the difference between upper limit sky map and the injected sky map.

even if the detectors are not sensitive enough to detect SGWB, the joint-index multi-component estimator provides safer upper limits when one cannot ignore the existence of more than one component.

11% of the points in the histogram fall under the negative region

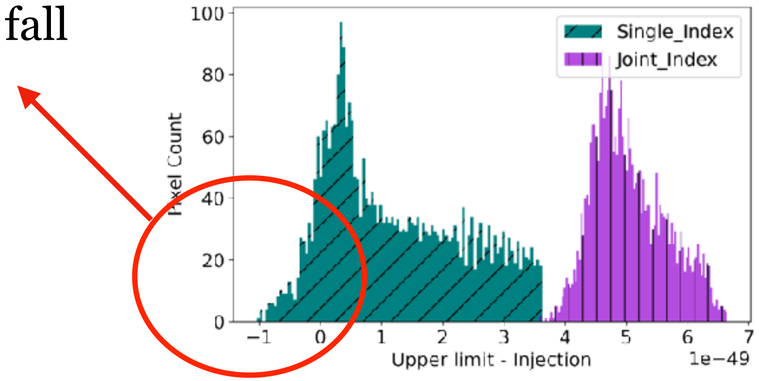

RADIOMETER SEARCH

Observed data:

$$C^I \equiv C^I_{ft} = \tilde{s}^*_1(t,f)\,\tilde{s}_2(t,f)$$

Noise (in the weak signal limit):

$$n^I \equiv n^I_{ft} = \tilde{n}^*_1(t,f)\,\tilde{n}_2(t,f)$$

Covariance matrix:

$$\mathcal{N}_{ft,f't'} = \mathsf{Cov}(C^I_{ft}, C^{I'}_{f't'}) \approx \frac{(\Delta T)^2}{4}\,\delta_{II'}\,\delta_{tt'}\,\delta_{ff'}\,P_2(t,f)\,P_1(t,f)$$

RADIOMETER SEARCH

To estimate the anisotropy of the SGWB, one can set up a likelihood function and then attempt to maximize it.

$$\mathscr{L} \propto \exp\left[-(C^{*}_{ft} - < C^{*}_{ft} >)\, \mathscr{N}^{-1}_{ft,f't'}\, (C_{f't'} - < C_{f't'} >)\right]$$

The maximum likelihood (ML) estimator of the SGWB anisotropy in the presence of additive Gaussian noise is then given by

$$\hat{\mathscr{P}} = \mathbf{\Gamma}^{-1}\, \mathbf{X}$$

Dirty Map —> Map of the SGWB convolved with the detector's response.

Clean Map —> Response of the detectors are deconvolved

Fisher Matrix —> Covariance matrix of the dirty map.

RADIOMETER SEARCH

The “narrowband dirty map” is given as

$$X_p(f) \;=\; \sum_{\mathcal{J}t} \frac{\gamma^{\mathcal{J}*}_{ft,p}\, C^{\mathcal{J}}(t;f)}{P_{\mathcal{J}_1}(t;f) P_{\mathcal{J}_2}(t;f)}\,,$$

Cross Spectral Density $\langle C^{\mathcal{J}}(t;f)\rangle \propto \hat{\mathcal{P}}(f,\hat{\mathbf{n}}_p)\,\gamma^{\mathcal{J}}_{ft,p}$

The noise covariance matrix in a weak signal limit is given by

$$\Gamma_{pp'}(f) \;=\; \sum_{\mathcal{J}t} \frac{\gamma^{\mathcal{J}*}_{ft,p}\,\gamma^{\mathcal{J}}_{ft,p'}}{P_{\mathcal{J}_1}(t;f)\,P_{\mathcal{J}_2}(t;f)}\,.$$

Where $\gamma^{\mathcal{J}}_{ft,p}$ is the direction-dependent overlap reduction function,

$$\gamma^{\mathcal{J}}_{ft,p} :\equiv \sum_{A} F^{A}_{\mathcal{J}_1}(\hat{\mathbf{n}}_p,t)\,F^{A}_{\mathcal{J}_2}(\hat{\mathbf{n}}_p,t)\,e^{2\pi i f\,\hat{\mathbf{n}}_p\cdot\Delta\mathbf{x}_{\mathcal{J}}(t)/c}$$

OVERLAP REDUCTION FUNCTION

Hanford-Livingston baseline

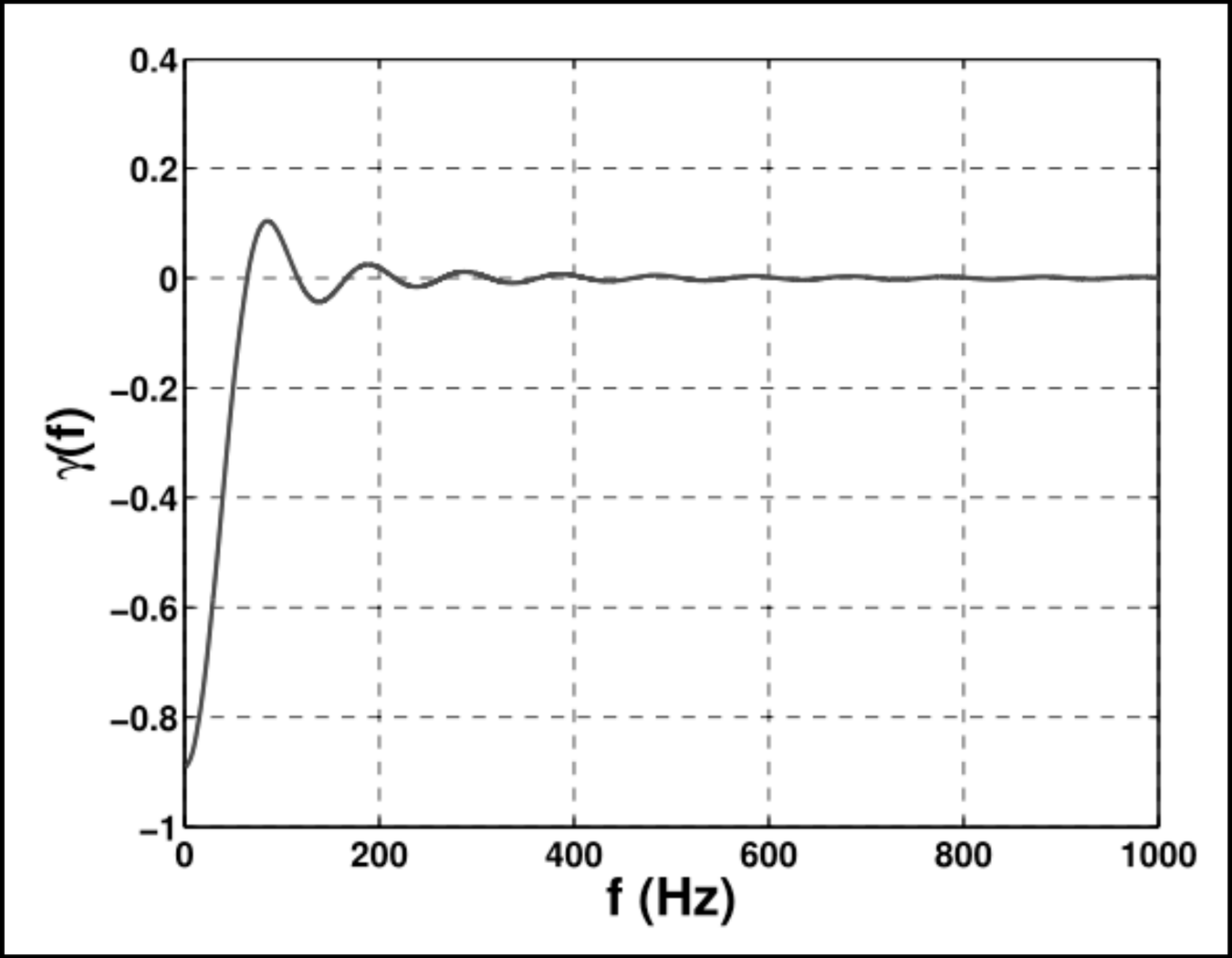

Negative values –> Detectors are rotated 90 degree relative the other.

Not -1 –> Two interferometers are not in the same plane.

Zeros–> At specific frequencies, we have no sensitivity to the gravitational waves

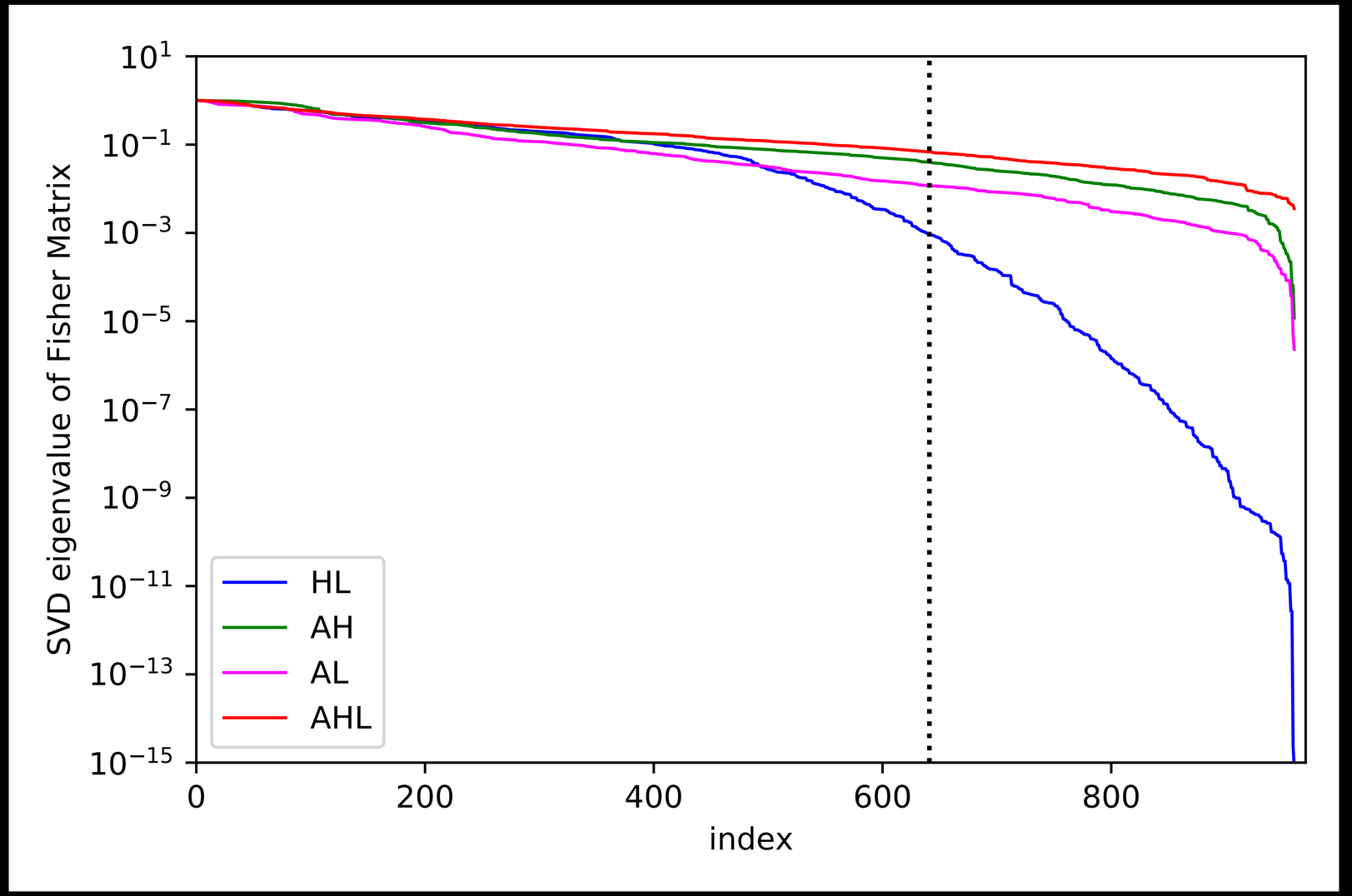
SVD eigenvalue of Fisher Matrix
10^{1}
10^{-1}
10^{-3}
10^{-5}
10^{-7}
10^{-9}
10^{-11}
10^{-13}
10^{-15}
0
200
400
600
800
index
HL
AH
AL
AHL